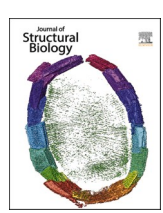
ELSEVIER

Contents lists available at ScienceDirect

# Journal of Structural Biology

journal homepage: www.elsevier.com/locate/yjsbi



# Research Article



# Morphological and genetic mechanisms underlying the plasticity of the coral *Porites astreoides* across depths in Bermuda

Federica Scucchia <sup>a,b,\*</sup>, Kevin Wong <sup>c</sup>, Paul Zaslansky <sup>d</sup>, Hollie M. Putnam <sup>c</sup>, Gretchen Goodbody-Gringley <sup>e,f,1</sup>, Tali Mass <sup>a,\*,1</sup>

- <sup>a</sup> Department of Marine Biology, Leon H. Charney School of Marine Sciences University of Haifa, Israel
- <sup>b</sup> The Interuniversity Institute of Marine Sciences, Eilat, Israel
- Department of Biological Sciences, University of Rhode Island, Kingston, United States
- <sup>d</sup> Department for Operative, Preventive and Pediatric Dentistry, Charité-Universitätsmedizin, Berlin, Germany
- e Central Caribbean Marine Institute, Little Cayman, Cayman Islands
- f Bermuda Institute of Ocean Sciences, St. George's, Bermuda

#### ARTICLE INFO

Edited by Bauke W. Dijkstra

Keywords: Coral reef Mesophotic X-ray micro-CT SEM RNA-Seq Climate refugia

#### ABSTRACT

The widespread decline of shallow-water coral reefs has fueled interest in assessing whether mesophotic reefs can act as refugia replenishing deteriorated shallower reefs through larval exchange. Here we explore the morphological and molecular basis facilitating survival of planulae and adults of the coral *Porites astreoides* (*Lamarck*, 1816; *Hexacorallia: Poritidae*) along the vertical depth gradient in Bermuda. We found differences in microskeletal features such as bigger calyxes and coarser surface of the skeletal spines in shallow corals. Yet, tomographic reconstructions reveal an analogous mineral distribution between shallow and mesophotic adults, pointing to similar skeleton growth dynamics. Our study reveals patterns of host genetic connectivity and minimal symbiont depth-zonation across a broader depth range than previously known for this species in Bermuda. Transcriptional variations across life stages showed different regulation of metabolism and stress response functions, unraveling molecular responses to environmental conditions at different depths. Overall, these findings increase our understanding of coral acclimatory capability across broad vertical gradients, ultimately allowing better evaluation of the refugia potential of mesophotic reefs.

# 1. Introduction

Tropical coral reefs have undergone global declines due to rapidly changing climate and the accumulation of anthropogenic local stressors (Pandolfi et al., 2011). Such losses are particularly marked in shallow reef systems of the Caribbean, that have a long history of increasingly stressful environmental conditions and dramatic coral losses (Cramer et al., 2021). Deeper reef systems (>30 m), also referred to as mesophotic coral ecosystems, represent potentially critical ecological refuges by offering shelter against disturbances and providing propagules to recolonize impacted shallow reefs (termed the Deep Reef Refugia Hypothesis - Bongaerts et al., 2010; Lesser et al., 2018). Although not ubiquitously immune to the impacts of disturbances (Appeldoorn et al., 2016; Bongaerts et al., 2013; Rocha et al., 2018; Smith et al., 2013), mesophotic coral ecosystems appear to be generally buffered from

bleaching and storm events (Bongaerts et al., 2010; Lesser et al., 2009; Pérez-Rosales et al., 2021), suggesting that increasing depth may offer a level of protection against shallow-water stressors.

The potential of mesophotic coral reefs to reseed shallower environments is tightly linked to the extent of species overlap across the vertical gradient. In the Caribbean region for example, 25 to 40% of coral species are depth-generalists, found along the depth gradient from shallow to mesophotic reef zones (Bongaerts et al., 2010). Such species overlap, however, does not necessarily ensure effective flow of larvae along the vertical gradient. Local adaptation, parental effects and larval selectivity could, in fact, pose a major ecological barrier to gene flow between shallow and mesophotic reefs (Shlesinger and Loya, 2021).

Light penetrating though the water column is an important selective factor for corals due to the dependence on the photosynthetic activity of algal endosymbionts for their energy requirements (Falkowski et al.,

<sup>\*</sup> Corresponding authors at: The Whitney Laboratory for Marine Bioscience, University of Florida, United States (F. Scucchia). *E-mail addresses*: federica.scucchia@studio.unibo.it (F. Scucchia), tmass@haifa.ac.il (T. Mass).

<sup>&</sup>lt;sup>1</sup> These authors contributed equally.

1984). Depth-generalist coral species have been found in association with different symbiont types across the vertical gradient (e.g. Bongaerts et al., 2015; Bongaerts et al., 2013) that are physiologically distinct having adapted, or acclimated, to different light conditions (Frade et al., 2008; Iglesias-Prieto et al., 2004). Such depth-zonation in symbiont species or phenotypes likely facilitates the distributions of coral hosts across broad vertical gradients (Frade et al., 2008). Other than symbiont photobiological features that optimize light-harvesting or photoprotective mechanisms, host morphological and physiological properties can also contribute to modulate the internal light field for their endosymbionts (Enríquez et al., 2005; Kramer et al., 2022a; Salih et al., 2000). For example, small-scale morphological changes result in greater self-shading and thus ensure that irradiance is kept at a photophysiological optimum in shallow Stylophora pistillata colonies, whereas the mesophotic skeletal architecture facilitates light capture by the endosymbionts (Kramer et al., 2022a). Such modifications of the coral skeletal morphology could be particularly advantageous in those cases where the hosted algal symbionts are not depth-specialists. In fact, if the Symbiodiniaceae consortia hosted by the coral colonies is similar regardless of depth, this could indicate that the coral-algal association is phenotypically flexible enough to be beneficial regardless of depthrelated environmental changes (Bongaerts et al., 2011). For vertically transmitting species (algal symbionts are transmitted from parent to offspring), hosting similar symbiont assemblages from shallow to mesophotic reefs may favor settlement of coral planulae across the depth gradient, as opposed to hosting depth-specialist symbionts that may function as a post-zygotic barrier to coral connectivity (Shlesinger and Lova, 2021).

The brooding coral Porites astreoides in Bermuda is one example of a coral species associated with the same dominant symbiont type (Symbiodinium type A4 or A4a) from the shallow to the upper mesophotic zone (Reich et al., 2017; Serrano et al., 2016). Other symbiont types have also been detected in P. astreoides across depths (type B - Breviolum and type C - Cladocopium, Reich et al., 2017) or exclusively in shallow corals (type B - Breviolum, Serrano et al., 2016). P. astreoides is commonly found throughout the Caribbean and Western Atlantic, occurring over a wide range of depths from 0 to 50 m (Fricke and Meischner, 1985). Several aspects make this species an ideal candidate to test the Deep Reef Refugia Hypothesis. In Bermuda, P. astreoides is a main contributor to reef community structure across the lagoon and rim reef zones (Goodbody-Gringley et al., 2019). From shallow to mesophotic reefs, this species exhibits similar thermal tolerance ranges and bleaching thresholds, despite the different thermal histories, suggesting high levels of plasticity to increasing temperatures (Gould et al., 2021). Earlier investigations have shown that *P. astreoides* populations maintain high levels of genetic connectivity in Bermuda from shallow to upper mesophotic zones (~25 m; Serrano et al., 2016). However, nothing is yet known about the genetic and phenotypic characteristics of P. astreoides at depths greater than 35 m for both adult and early life history stages.

Previous studies have assessed phenotypic changes that allow certain coral species to thrive across broad depth distributions, such as modifications of skeletal morphology (Goodbody-Gringley and Waletich, 2018; Malik et al., 2020; Studivan et al., 2019), physiology (Goodbody-Gringley et al., 2021; Mass et al., 2007; Scucchia et al., 2021, 2020) and photobiology (Carpenter et al., 2022; Einbinder et al., 2016; Lesser et al., 2010; Martinez et al., 2020). However, there is a general lack of knowledge about the molecular mechanisms that underlie such phenotypic variations across depths for most coral species. Only a few studies in fact have attempted to uncover gene expression patterns and major biological pathways that contribute to the persistence of depthgeneralist corals from shallow to mesophotic reefs (Malik et al., 2020; Scucchia et al., 2021; Studivan and Voss, 2020). Importantly, the focus of these studies has been put on adult corals, while little is currently known about gene expression dynamics in early life stages of corals across vertical gradients. Thus, the genetic basis that could facilitate migration and settlement of coral planulae to different depth zones remains poorly understood.

In this study, we examined skeletal, genetic and transcriptomic patterns of P. astreoides planulae and adults from shallow ( $\sim$ 10 m) and mesophotic ( $\sim$ 45 m) reefs in Bermuda. We provide an assessment of the biological processes that facilitate coral plasticity along differing environmental conditions at depth. Elucidating the mechanisms contributing to the persistence of different coral life stages across broad depth gradients will ultimately allow us to better evaluate the capacity of coral planulae to disperse across depths, shedding light on the potential for mesophotic reefs to serve as refugia in the face of global environmental change.

#### 2. Materials and methods

#### 2.1. Site selection and sample collection

Two study sites on the north Atlantic Bermuda platform were selected for this study: a rim reef (Hog Shallow; 8–10 m depth;  $32^{\circ}27'26''N$ ,  $64^{\circ}50'05''$  W), and a mesophotic reef (Hog Deep; 45 m depth;  $32^{\circ}29'18''$  N,  $64^{\circ}51'18''$  W)(Fig. S1), located at 4.3 km from each other. Throughout the summer temperatures were found to be consistently higher at shallower depth, with maximum temperature at the shallow site peaking at  $28.9^{\circ}C$ , compared to  $26.8^{\circ}$  C at the mesophotic site (Goodbody-Gringley et al., 2021).

A total of 20 adult colonies of the coral *P. astreoides* were randomly chosen and collected using a hammer and chisel (PSLicenses #2019061407): 10 from the shallow reef ( $\sim$ 10 m depth) and 10 from the mesophotic reef ( $\sim$ 45 m depth), 9 days prior to the July new moon (22 July 2019) based on previous data documenting larval release beginning up to 10 days prior to the full moon (de Putron and Smith, 2011). At each site, a fragment of  $\sim$ 2 cm² was collected from 3 adult colonies on the boat directly after collection from the reef and was immediately stored in DNA/RNA Shield (Zymo Research) for molecular analysis. Additional  $\sim$ 2 cm² fragments were collected from each colony per each site and stored with ethanol for scanning electron microscope (SEM) and X-ray  $\mu$ CT analysis.

To enable planulae collection, adult corals retrieved from the reef were transferred to the outdoor mesocosm at the Bermuda Institute of Ocean Sciences (BIOS) where they were maintained under ambient temperature conditions in 400-L flow tanks using seawater pumped directly from the adjacent shoreline, that is exposed to moderate flow and frequent turnover from the open ocean. Temperature was recorded in the mesocosm tanks daily using a HOBO onset data logger on 1-min intervals (27.6 °C  $\pm$  0.004, shallow; 27.5 °C  $\pm$  0.005, mesophotic; mean  $\pm$  SEM). To reduce light stress and maintain temperature controls, water level heights of ~45 cm above the colony surface were maintained during the day. All corals experienced a natural light period as no artificial light source was provided and the mesocosm facility is exposed to natural light with no coverings that block incoming light. Mesophotic colonies were covered with a single layer of light filter (Lagoon Blue, LEE Filters) to mimic mesophotic light levels, while shallow colonies were left uncovered. Daily light readings using a PME miniPAR logger were recorded for each condition over the period that corals were in the mesocosm (10 days), as previously detailed (Goodbody-Gringley et al., 2021). In situ light measurements from the collection sites were taken every 30 s for a period of 3-4 min at depths of 10 m and 45 m on the day of coral collections using a Li-COR sensor on a stable frame with a 100 m fiber optic cable. During the daily timing of highest light exposure (12:00 – 13:00) over the period of time the corals were in the mesocosm (10 days), mean light in the mesophotic condition tank was 139 + 0.89 $\mu$ mol/s m<sup>2</sup>, compared to a mean level of 124 + 0.16  $\mu$ mol/s m<sup>2</sup> recorded over the same period and time of day in situ, and 442 + 36.9  $\mu mol/s \ m^2$ in the uncovered (shallow conditions) tanks, compared to 392 + 0.92μmol/s m<sup>2</sup> in situ. All light measurements were reported in (Goodbody-Gringley et al., 2021).

Larval P. astreoides collections were accomplished from July 24 to

July 26, 2019. During the larval collection period, tank water levels were dropped at night and individual colonies were placed into 2-L plastic separated jugs with individual lines of flowing seawater. An 800 mL polypropylene beaker with a 153 µm mesh bottom was placed under the spout of each container to collect the positively buoyant planulae following the methods of (Goodbody-Gringley et al., 2018). Every morning at dawn, all planulae released from each colony were collected with a sterile clear transfer pipette and pooled by reef depth to randomize larval selection among parental colonies. Subsamples were then immediately taken from the pooled planulae and placed in 1.5 mL tubes (3 tubes per depth of origin, ~20 planulae per tube) and stored with DNA/RNA Shield (Zymo Research) for molecular analysis.

#### 2.2. Adult skeletal micromorphology

Adults fragments collected at each depth that were stored with ethanol were immersed in 1% sodium hypochlorite (NaClO) for 10 min to remove the living tissue. Thereafter, the skeletons were rinsed with distilled water followed by drying overnight. Fragments were vacuum coated with gold (for conductivity) prior to examination under a ZEISS SigmaTM SEM (Germany), by using an In-lens detector (2 kV, WD = 3–4 mm). In each fragment, the area of the calyx of individual polyps (N = 15) was measured with the image processing package FIJI (Schindelin et al., 2012) delimiting and selecting the calyx region in the SEM images. The number of rapid accretion deposits (RADs) on the skeletal spines (N = 12) was measured as the ratio between the number of RADs to surface area of the spine, calculated using FIJI (Schindelin et al., 2012) and following the method by Scucchia et al., 2021.

#### 2.3. X-ray µCT: Image acquisition and tomographic reconstruction

Tomographic scanning was conducted at BAMline (Görner et al., 2001), the imaging beamline of BESSY II (the synchrotron storage ring of HZB-Helmoholtz-Zentrum Berlin, Germany) on the adult skeleton fragments. Each sample was attached to a stub and scanned with incremental rotation (multiple projections spanning 360°) on a high-resolution imaging sample stage (Zaslansky et al., 2011) with exposure times set to 140 ms. Projection images were acquired with a final pixel size of 3.61  $\mu m$ , using an energy of 24.5 keV.

Prior to reconstruction, data were normalized to account for beam inhomogeneities using FIJI (Schindelin et al., 2012) in the laboratory of the Charité, Universitätsmedizin (Berlin, Germany). Specifically, for each scan, the radiograms were background-corrected by normalization with empty beam (flat-field) images, obtained both before and after each scan. Reconstruction was performed by the filtered back projection method using nRecon (v1.7.4.2, Brucker micro-CT, Kontich, Belgium). Tomographic datasets were visualized and further processed in 3D using Dragonfly (v2021.3, Object Research Systems-ORS, Montreal, Quebec, Canada)(Makovetsky et al., 2018). For each reconstructed fragment, the volumetric thickness of the skeleton was computed using the "Create Volume Thickness Map" function built into Dragonfly, which performs volume thickness measurements based on the sphere-fitting method. Specifically, the skeletal thickness is computed per each tomographic slice within and between single polyps, taking into account the skeletal macro-porosity (holes and crevices between polyps, see Fig. S2). Such measurement is carried out per each tomographic slice across the entire skeletal sample, allowing examination of the skeletal deposition pattern at the macro-scale in the newest layers of the skeleton.

#### 2.4. RNA extraction and sequencing

Total RNA was extracted from the planulae (pools of  $\sim\!20)$  and adult samples (that were stored with DNA/RNA Shield) using the Invitrogen PureLink RNA micro (for the planulae) and mini (for the adults) kits according to the manufacturer's protocol (Thermo Fisher Scientific). DNAase treatment was performed within the RNA extraction procedures

according to the Invitrogen PureLink RNA kit instructions. RNA concentration was confirmed using a NanoDrop 2000 (Thermo Fisher Scientific, United States) and quality was tested on a TapeStation (Agilent Technologies, United States); only samples with RNA integrity number values above 8 were selected for sequencing.

Three independent samples were obtained for each developmental stage and depth of origin. Strand-specific RNA-seq libraries were prepared using an in-house protocol at the Weizmann Institute of Science (Israel). Briefly, mRNA was captured via polyA selection from 500 ng of total RNA followed by fragmentation and the generation of double-stranded cDNA. Then end repair, A base addition, adapter ligation and PCR amplification steps were performed. Sequencing libraries were constructed with barcodes to allow multiplexing of all samples to be run in each lane. Paired-end reads (100 bp) were sequenced on an Illumina NovaSeq 6000 across two different lanes (i.e., each sample run on each lane to remove batch effects and the sequence files were concatenated for analysis).

# 2.5. RNA-Seq reads alignment to reference genome and symbiont species identification

Read quality of raw RNA-Seq was assessed using FastQC (v0.11.9) and compiled with MultiQC (v1.10.1). Reads were then trimmed and filtered using Cutadapt (v2.6, Martin, 2011) and Trimmomatic (v0.39, Bolger et al., 2014), to retain reads with and average quality score of at least 25. Reads were then aligned to the P. astreoides host genome assembly (Wong and Putnam, 2022)(assembly as well as structural and functional annotation data are available at DOI https://doi.org/10.1760 5/OSF.IO/ED8XU, NCBI Accession PRJNA834048) using HISAT2 (v2.2.1, Kim et al., 2019) in the stranded paired-end mode and assembled using StringTie (v2.2.5, Pertea et al., 2015). GFFcompare (v0.12.2, Pertea and Pertea, 2020) was used to assess the precision of mapping by comparison of merged mapped GFFs to the P. astreoides reference assembly. Finally, a gene count matrix was generated using the StringTies python script prepDE (Pertea et al., 2015). To identify algal symbiont species, high-quality reads were subjected to a BLASTx search using Diamond (v2.0.11, Buchfink et al., 2015) against open-access genomebased proteome databases of Symbiodiniaceae species (Table S1).

# 2.6. Coral host single nucleotide polymorphisms and FST analyses

Single nucleotide polymorphisms (SNPs) were extracted from the RNA-Seq data using the Genome Analysis Toolkit framework (GATK, v4.2.0; McKenna et al., 2010) following the recommended RNA-Seq SNPs practice of the Broad Institute (Auwera et al., 2013), with necessary adjustments for genotype calling in non-model organisms where variants sites are not known beforehand, since calibration of GATK SNP calling parameters is largely dependent on known variant datasets (Auwera et al., 2013). In short, HISAT-aligned reads were sorted and marked for duplicates, variant calling was performed with the GATK HaplotypeCaller tool (McKenna et al., 2010) and genotypes were then jointly called using the GATK GenotypeGVCFs tool. The GATK Select-Variants and VariantFiltration tools were used to filter the joined variantcalling matrices for quality by depth, producing a filtered genotype matrix of ~400,000 SNPs. Finally, filtering for linkage disequilibrium was applied using the –indep-pairwise function of PLINK (v2.0, Purcell et al., 2007); producing a final genotype matrix of 12 individuals and 9,060 SNPs.

To assess genetic differentiation among age-depth groups, the genotype matrix was loaded as a Genomic Data Structure (GDS) object in the R environment (v3.6.3, R Core Team, 2020) using the function snpgdsOpen of the package SNPRelate (v1.20.1, Zheng et al., 2012). The fixation index (F<sub>ST</sub>, Weir and Cockerham, 1984) was estimated using the package HIERFSTAT (v0.5.10), and resulting F<sub>ST</sub> pairwise values were tested for significance with 999 permutations.

#### 2.7. Host differential gene expression analysis and WGCNA

Within the R environment (v3.6.3, R Core Team, 2020), the gene count matrix was filtered to remove low-counts genes using the *pOverA* filter function of the package Genefilter (v1.68.0). Specifically, genes with less than 10 counts in at least 3 (minimum number of replicates per each condition) out of 12 samples were excluded. Counts were then normalized using the variance stabilizing transformation (vst) in DESeq2 (v1.26.0, Love et al., 2013) and PCA was conducted using the *plotPCA* function to calculate sample-to-sample distances. Differential expression analysis with DESeq2 was performed between depths (mesophotic and shallow) for each life stage (planulae and adults) using the Wald test (Love et al., 2014), to identify differentially expressed genes (DEGs) with adjusted p-value (FDR, < 0.05).

Normalized counts (vst-transformed) were also used to perform Weighted Gene Co-expression Network Analysis (WGCNA)(Langfelder and Horvath, 2008) to identify modules (groups of genes) with different expression profiles across depths but with similar expression between life stages at the same depth. Compared with focusing solely on DEGs, WGCNA makes use of the expression data of all genes to identify gene modules of co-expression and therefore enables association analysis (e. g., correlation) with the phenotypes under study. First, an unrooted hierarchical tree was built using the R function hclust "average" to check for outliers. The function pickSoftThresholding of the WGCNA package (v1.70.3) was used to explore values of soft threshold from 1 to 30, to construct a topological overlap matrix similarity network and assess gene expression adjacency (Langfelder and Horvath, 2008). A soft thresholding power of 17 was chosen (scale-free topology fit index of 0.8) and used to construct the topological overlap matrix similarity network with adjacency of type "signed", which is used to keep track of the sign (negative or positive) of the co-expression information (Langfelder and Horvath, 2008). The WGCNA package dynamicTreeCut was used to identify modules from the topological overlap matrix similarity network with minimum module size of 30, producing a total of 103 modules. Modules with >85% eigengene similarity were merged, resulting in a total of 56 finalized modules.

The hclust "average" method was used to cluster the expression modules by eigengene similarity, and module-trait correlation was assessed by determining the genes significance (correlation between genes and age-depth groups) and the module membership (correlation between modules eigengene and genes expression profiles)(Langfelder and Horvath, 2008). The module-trait correlation values were plotted as a heatmap with the package *complexHeatmap* and the 56 modules were divided into clusters with the function row\_split of complexHeatmap to highlight changes in expression by age-depth. Finally, the expression profile in each cluster of modules was summarized by generating plots of mean eigengene expression value per each age-depth group. The variation in mean eigengene expression of each cluster was analyzed using Mann Whitney test within the comparisons mesophotic versus shallow adults and mesophotic versus shallow planulae. The rationale for the Mann Whitney test is to detect module clusters that share the same upor down-ward trend of expression across developmental stages of corals at the same depth (i.e., finding module clusters that show a depthdependent pattern across developmental stages), and to find module clusters that have an opposite trend between corals of the same age but from different depths (i.e., finding module clusters that show a depthdependent pattern at different developmental stages).

# 2.8. Host gene ontology enrichment analysis

Gene Ontology (GO) enrichment analysis was performed to examine functions and processes primarily related to each depth across developmental stages, converting both DEGs and WGCNA modules into biological knowledge. First, GO annotation of the *P. astreoides* genome was retrieved from the work of Wong and Putnam (Wong and Putnam, 2022). GO enrichment analysis was performed using the package Goseq

(v1.42.0, Young et al., 2010) in the R environment. For the enrichment analysis based on the DE data, several cut-offs on the number of DEGs to be used were tested, to ensure obtaining a reasonable number of enriched GO terms. Specifically, for both the mesophotic versus shallow adults and planulae comparisons, only DEGs with log2FoldChange>|2| were included in the analysis. Furthermore, the list of significantly enriched GO terms of the mesophotic versus shallow planulae comparison was filtered before final plotting by only keeping terms with at least 2 DEGs per category (numDEInCat) and by excluding broader terms such as "modulation process of other organism", "membrane", "component of membrane" that may be less informative. After filtering, enriched GO terms were hierarchically clustered based on pairwise distances between groups of genes and a terms tree was constructed using the clustering method "Ward" with the package Bioconductor-ggtree (Yu et al., 2018) as described previously (Malik et al., 2020; Scucchia et al., 2021). The full list of enriched GO terms is available in the electronic notebook https://github.com/fscucchia/Pastreoides development depth.

For the WGCNA data, only the modules clusters with the same direction of change and with highly significant (p < 0.001) differences in mean eigengene expression in both the between-adults and betweenplanulae comparisons were included in the GO enrichment analysis. Since a large number of enriched GO terms resulted to be significant within each cluster of modules (range of ~300-1500 significant GO terms per cluster), the stringent significance cutoff of p < 0.001 was chosen to identify clusters of modules with the highest relatedness to changes in the trait of interest (depth) between groups. The package Goseq (v1.42.0, Young et al., 2010) was used to perform the enrichment analysis. For the resulting enriched GO terms, slim categories were obtained with the function goSlim of the R package GSEABase (v1.52.1) using the GOslim generic obo as reference database (v1.2, Ashburner et al., 2000). The full list of WGCNA-related enriched GO terms is available in the electronic notebook https://github.com/fscucchia/ Pastreoides\_development\_depth.

# 2.9. Statistical analysis

The mean thickness value per each skeleton fragment (N = 3 fragments per depth), the area of the calyxes (N = 15 calyxes per depth) and the number of RADs per unit surface area of the spines (N = 12 per depth) were tested for normality (Shapiro–Wilk test) and homogeneity of variance (Brown–Forsythe test). For the skeletal thickness and the calyx area, an unpaired t-test was used, whereas Mann-Whitney test was used for the RADs number (to test the differences between depths), in which significant groups have a value of p  $\leq$  0.05. GraphPad Prism version 9.0.0 (GraphPad Inc., San Diego, CA, USA) was used to perform the statistical tests.

#### 3. Results

#### 3.1. Adult skeletal growth patterns

We characterized adult colony structure and various micro-scale skeletal features associated with living in shallow or mesophotic reef environments. Scanning electron microscope (SEM) observations show that the area of the corallites significantly decreased from 2.23 mm² in shallow corals to 1.54 mm² in mesophotic corals (unpaired *t*-test, N = 15, p < 0.001)(Fig. S3a). Furthermore, mesophotic adults appear to possess a less extensive development of RADs on the spines (2.13  $\pm$  0.05, average number of RADs/mm²), which appear to be smoother compared to shallow adults (2.80  $\pm$  0.04 RADs/mm²) (Mann-Whitney test, N = 12, p < 0.001) (Fig. 1a-d and Fig. S3b). However, surface micro-texture examinations reveal that the aragonite crystal morphology was highly similar at both depths, characterized by bundles of fibers ranging between rhomb-shaped structures and flat blades (Fig. 1e, f).

Further morphological investigations were conducted by imaging adult fragments with X-ray µCT (Fig. 2). Three dimensional renderings

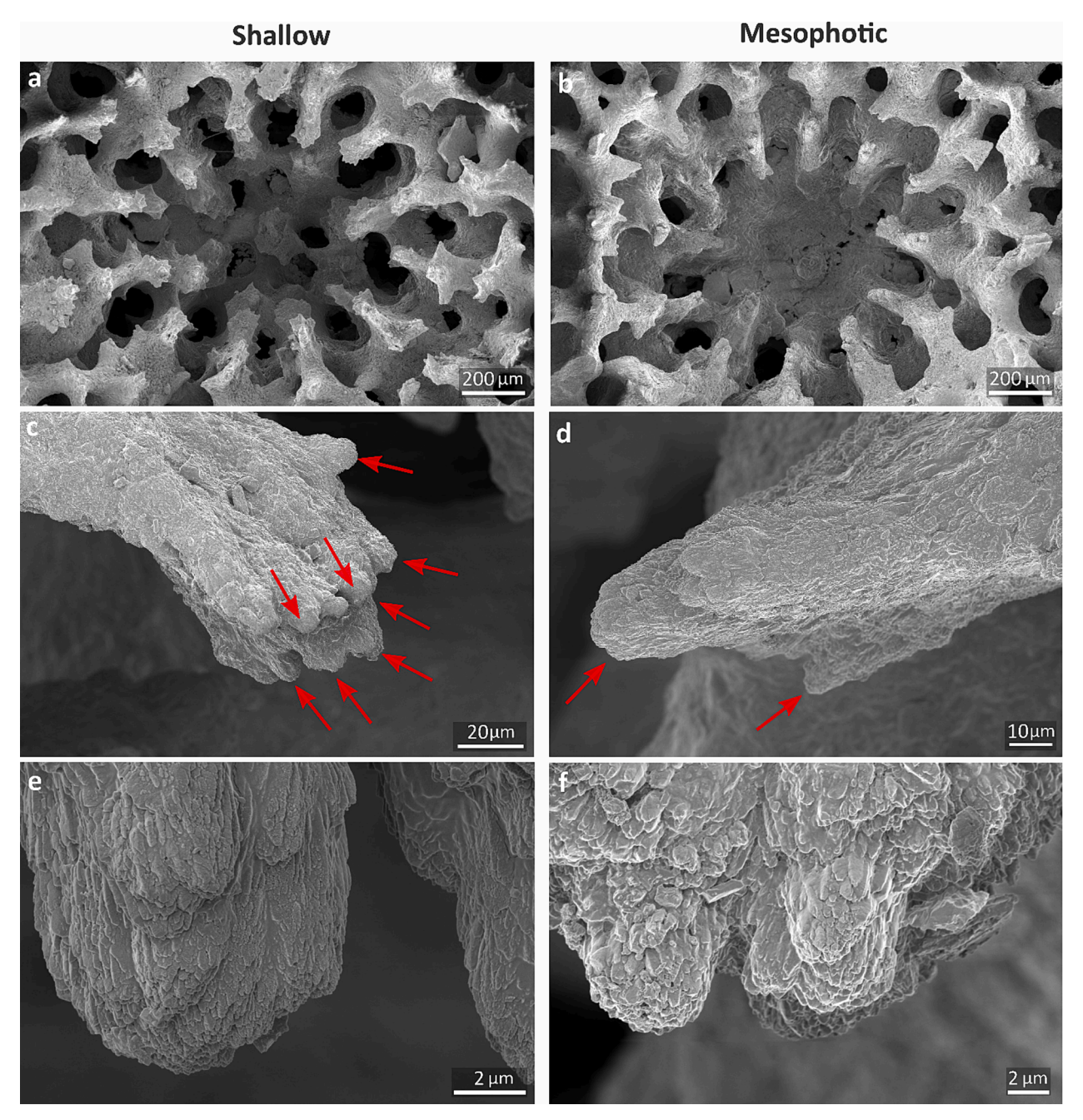


Fig. 1. Comparison between skeletal features of shallow and mesophotic adult *P. astreoides* corals. (a, b) SEM images showing typical calyxes and spines structure; (c, d) enlargements showing the rapid accretion deposits (RADs; globular elements indicated by red arrows) on the spines surface and (e, f) enlargements showing the spines surface texture in shallow and mesophotic *P. astreoides* polyps. (For interpretation of the references to color in this figure legend, the reader is referred to the web version of this article.)

of the skeleton volumetric thickness show the distribution of the mineral both within and between single corallites in mesophotic and shallow corals (Fig. 2b, d; Movie S1 and S2). Single tomographic cross-sectional slices (Movie S1 and S2) and sliced top-view 3D renderings (Fig. 2f, h) reveal the internal architecture of the skeleton at both depths. Measurements of the overall mean skeletal thickness distributions do not show any significant differences between shallow and mesophotic adults (unpaired t-test, N = 3, p = 0.8)(Fig. 2e, g, Fig. S4).

# 3.2. Host genetic connectivity and identification of symbiont identities

We next aimed to elucidate whether the patterns we observed in the skeleton result from morphological plasticity or genetic adaptation. For that, we assessed the vertical genetic connectivity between shallow and mesophotic P. astreoides corals by estimating the fixation index  $F_{ST}$  from transcriptome-derived SNPs. Overall, pairwise  $F_{ST}$  estimates support genetic connectivity between shallow and mesophotic conspecifics, corresponding to  $F_{ST}=0.051$  (p <0.05) between P. astreoides adults (Fig. 3a). Relatively higher differentiation exists between mesophotic and shallow planulae (0.107, p <0.05) than between adults, possibly due to the fact that each planulae sample corresponds to a pool of planulae generated from different adult colonies.

Symbiont species identification analysis reveals that planulae and adults from both depths host a similar consortium of *Symbiodinium* species (*Symbiodinium* CladeA3, *Symbiodinium microadriaticum*, *Symbiodinium linucheae*; Fig. 3b). Among these symbiont species, *Symbiodinium* 

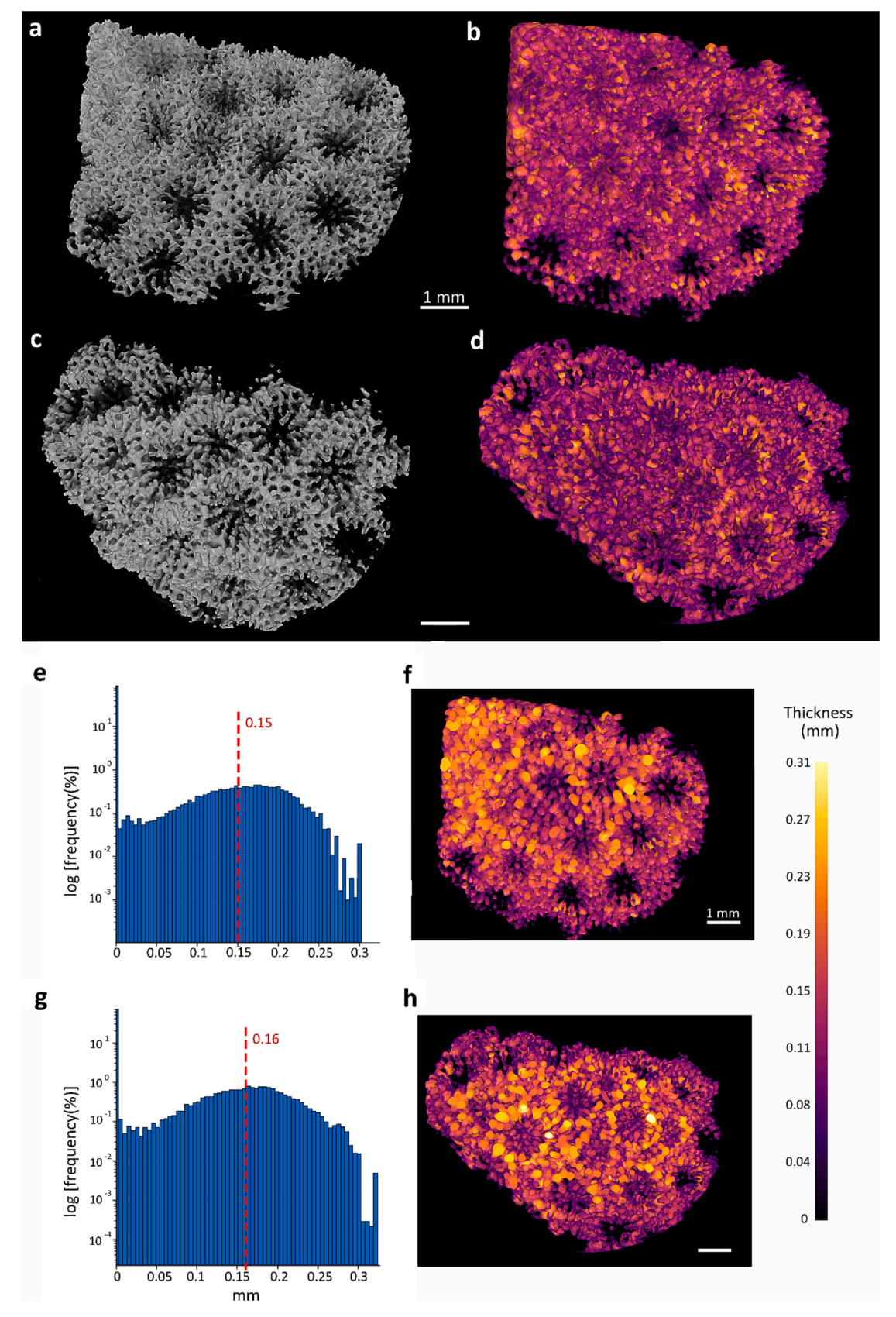
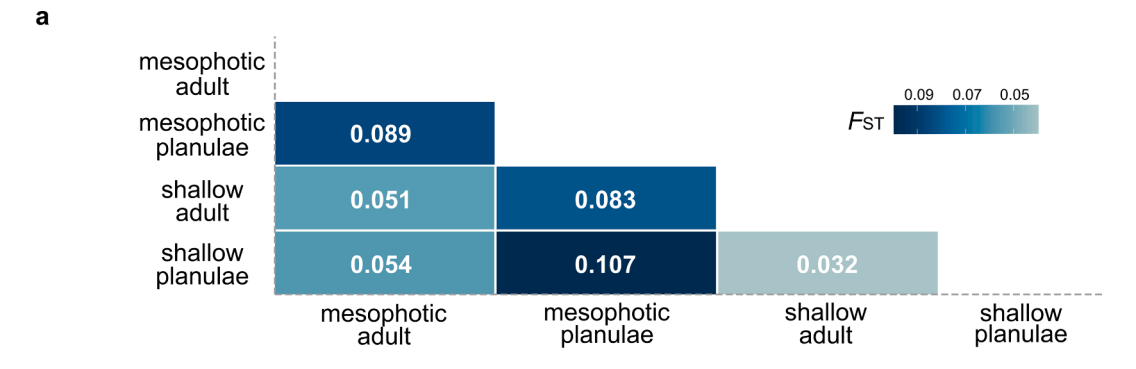


**Fig. 2. Volumetric thickness distribution in shallow and mesophotic** *P. astreoides* **corals.** 3D renderings of skeleton fragments (a, c) before and (b, d) after applying volume thickness analysis of (a, b) shallow and (c, d) mesophotic corals. (e, g) Frequency distribution of thickness values in (e) shallow and (g) mesophotic and (f, h) sliced top-view 3D renderings showing the internal thickness distribution in (f) shallow and (h) mesophotic. Red dotted lines indicate the mean thickness value per each skeleton fragment in (e, g). Thickness values are 2 dimensional measurements of the thickness of each voxel (volume pixel) in the fragments being measured. (For interpretation of the references to color in this figure legend, the reader is referred to the web version of this article.)

b



proportion of BLASTed reads

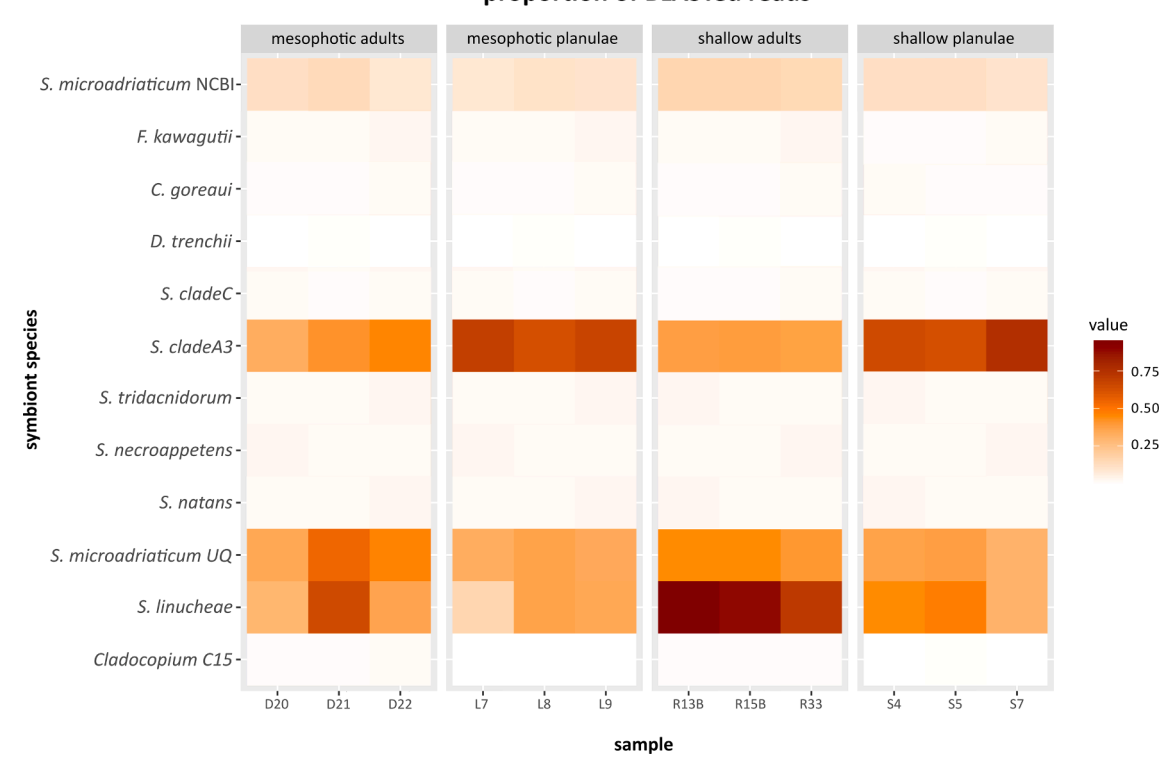


Fig. 3. Host genetic differentiation and algal symbiont species identification. (a) Genetic differentiation of the coral host as measured by fixation index ( $F_{ST}$ ). The pairwise  $F_{ST}$  statistic was calculated based on polymorphic transcriptome-derived SNPs. The level of dissimilarity among shallow and mesophotic planulae/adults is shown in increasing intensities of blue. (b) Species origin of symbiont sequences were detected by performing a BLASTx search using high-quality reads against open-access proteome databases of Symbiodiniaceae species (see Table S1). (For interpretation of the references to color in this figure legend, the reader is referred to the web version of this article.)

*linucheae* appears to be more abundant in shallow adults, where approximately 85% of all reads BLASTed against Symbiodiniaceae species belonged to *S. linucheae*, whereas in mesophotic adults only 43% of all reads belonged to the same symbiont species.

#### 3.3. Host gene expression patterns

We explored the genomic basis of phenotypic variation across diverse environments by examining the association of gene expression with environmental condition. A principal coordinate analysis conducted on expressed genes of P. astreoides planulae and adults reveals a much tighter clustering of shallow corals compared to their mesophotic conspecifics (Fig. 4a and 4b). Out of a total 24,247 expressed genes, 1.8% (439 genes) were found to be differentially expressed (P < 0.05) between mesophotic and shallow adults (Fig. 4c). In planulae samples, out of 32,724 expressed genes 8.9% (2,898 genes) were found to be differentially expressed (Fig. 4d).

Rather than focusing solely on the expression of individual genes, adaptation to shallow and mesophotic depth environments was additionally investigated by looking at co-expression patterns using Weighted Correlation Network Analysis (WGCNA)(Langfelder and Horvath, 2008). All expressed genes across coral samples were assigned by WGCNA into 56 modules, that showed ten distinct expression profiles (Fig. 5a). Significant (p < 0.05) module-trait correlations were found for 14 modules in mesophotic adults, 13 modules in shallow adults, 3 modules in mesophotic planulae and 5 modules in shallow planulae. No modules were found to share the same up- or down-ward trend of expression across developmental stages of corals at the same depth (i.e., no modules specific to shallow or mesophotic depth environments across developmental stages were observed).

The overall expression of genes in each module cluster was summarized by mean module's eigengene value (Fig. 5b). No clusters were found with significant adult-planulae co-variance in mean eigengene value due to depth origin, but 6 clusters showed a significant difference

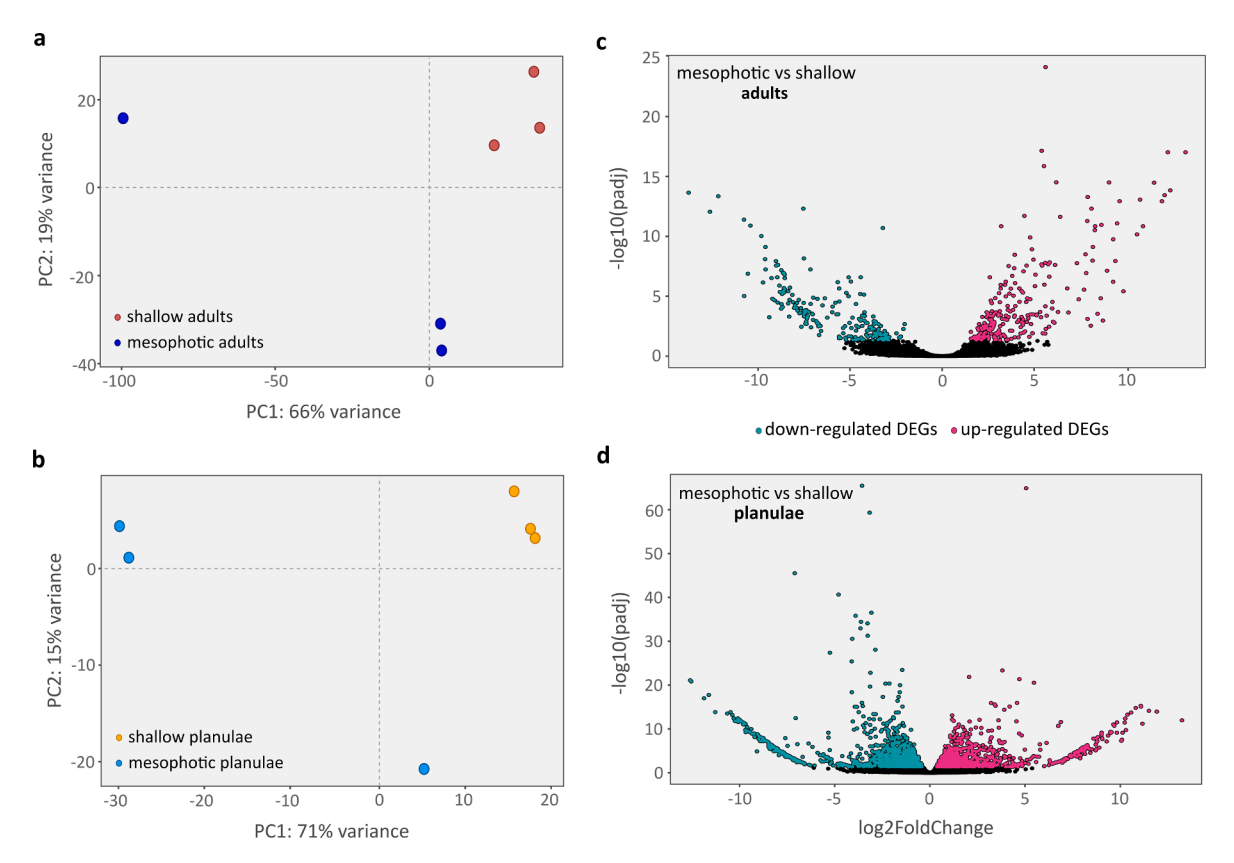


Fig. 4. Differential gene expression analysis results. (a, b) Principal component analysis (PCA) plots of the normalized expression matrix of the (a) mesophotic versus shallow adult comparison and of the (b) mesophotic versus shallow planulae comparison. (c, d) Volcano plots showing the corresponding differentially expressed genes (DEGs) for the (c) adults and (d) planulae comparisons. Green and pink dots denote significantly (p < 0.05) down-regulated and up-regulated genes, respectively. (For interpretation of the references to color in this figure legend, the reader is referred to the web version of this article.)

in eigengene expression due to depth origin in either the adults or planulae comparisons. Specifically, mean eigengene values were significantly different between adults in clusters 3, 4 and 5, and between planulae in clusters 7, 8 and 10. Between these, the most significant differences were found in clusters 5 (Mann Whitney test, N=24, p<0.001) and 7 (Mann Whitney test, N=9, p<0.001).

# 3.4. Host gene ontology enrichment

Enrichment analysis performed on DEGs resulted in 20 overrepresented GO terms in the within-adults comparison, and 29 GO terms in the within-planulae comparison (Fig. 6). Genes associated with GO terms involved in peptidases activity ("peptidase inhibitor activity" GO:0030414, "negative regulation of endopeptidase activity" GO:0010951, "metalloendopeptidase inhibitor activity" GO:0008191, "negative regulation of peptidase activity" GO:0010466) were upregulated in mesophotic corals compared to shallow corals for both planulae and adults, showing a depth-dependent pattern across developmental stages (Fig. 6). In addition, genes associated with terms involved in immune response ("immune response" GO:0006955, "tumor necrosis factor" GO:0005164) were downregulated in mesophotic corals compared to their shallow counterparts in both planulae and adults. In the within-planulae stage comparison, genes associated with the "ATPase activity" (GO:0016887) GO term were downregulated in mesophotic planulae as compared to the shallow ones, whereas genes linked to the terms "oxidoreductase activity" (GO:0016702), "actin binding" (GO:0003779), "lipid binding" (GO:0008289), "peptide metabolic process" (GO:0006518), "nematocyst" (GO:0042151) and "toxin activity" (GO:0090729) were upregulated in mesophotic planulae (Fig. 6).

In addition, gene ontology enrichment analysis undertaken for WGCNA module clusters showed highly significant differences in mean eigengene expression values between mesophotic and shallow corals in the case of adult samples (cluster 5) and planulae samples (cluster 7) (Fig. 5b). A total of 1758 GO terms were found to be over-represented in cluster 5 (Fig. 7), with a negative module-trait correlation in mesophotic adult corals and a positive correlation in shallow adult corals (Fig. 5b). These terms are primarily related to 65 slim terms, including anatomical structure development, signaling, immune system process, ribosome biogenesis, carbohydrate metabolic process, lipid metabolic process and lipid binding, inflammatory response and circulatory system process (Fig. 7). In cluster 7, a total of 253 were over-represented (Fig. 7) with a negative module-trait correlation in mesophotic planulae and a positive correlation in shallow planulae (Fig. 5b). Biological processes and molecular functions of cluster 7 were summarized by 33 slim terms, including anatomical structure development, signaling, immune system process, lipid metabolic process, vitamin metabolic process, protein catabolic process, membrane and cytoskeleton organization, cell differentiation, carbohydrate metabolic process and transporter activity (Fig. 7).

# 4. Discussion

In this study, we uncovered the phenotypic flexibility of the coralalgal association that contributes to the persistence of *P. astreoides* corals across broad vertical gradients, from shallow to mesophotic reefs. Several coral skeletal features are implicated in light collection or dissipation due to light-driven morphological plasticity. The coarser surface of the skeletal spines in shallow *P. astreoides* adults (Fig. 1a, c) suggests a higher dissipation of excess light through self-shading skeletal features, whereas the smoother spine surfaces in mesophotic adults (Fig. 1b, d) indicate a light-passage-facilitating functional trait. Such morphological patterns have also been observed between shallow and

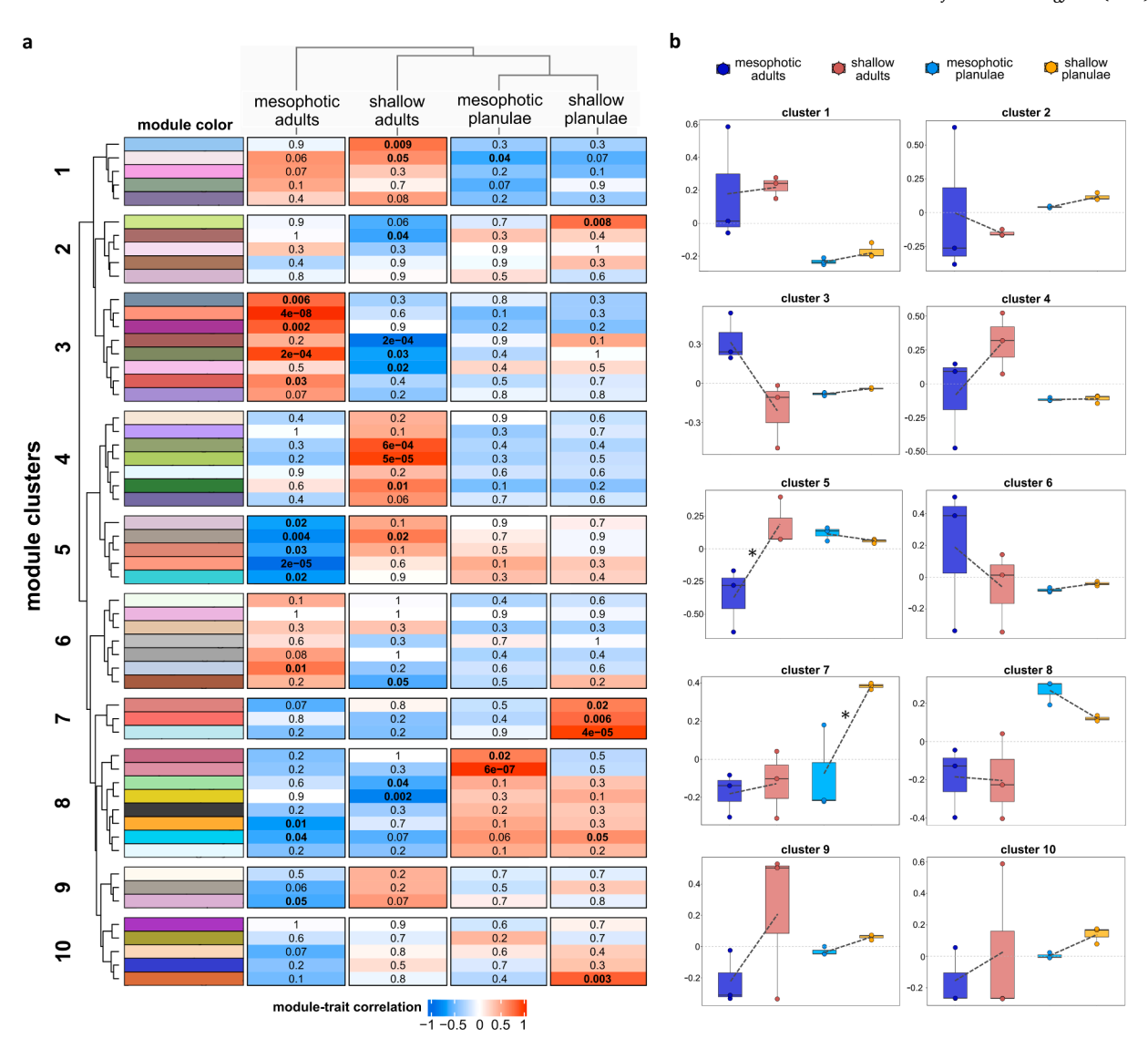


Fig. 5. Identification of clustered module-trait correlations by WGCNA analysis. (a) Clustered heatmap showing correlations between modules and age-depth groups. The module color is shown on the left side of each row. In total, 56 modules are shown, grouped into 10 clusters. Values of correlation between each module and the different clustered age-depth groups (mesophotic adults, shallow adults, mesophotic planulae, shallow planulae) range from -1 (anti-correlation) to +1 (positive correlation). Statistically significant (p < 0.05) correlation values are shown in bold. (b) Boxplots of mean eigengene expression value of each age-depth group for each WGCNA module cluster shown in (a). Each dot in the boxplots represents one sample (n = 3 per group), the dotted black lines show the degree of change between mean eigengene expression values among depths (within the same age group). Asterisks indicate highly significant (p < 0.001) differences in mean eigengene expression values between mesophotic and shallow adults (cluster 5) and planulae (cluster 7).

mesophotic *S. pistillata* adults in the Red Sea (Malik et al., 2020). Adjustments of coral skeletal traits to their ambient light conditions have been suggested to complement the endosymbionts demands for light, resulting in significantly higher light absorption in mesophotic corals compared to their shallow counterparts (Kramer et al., 2022a, 2022b).

*P. astreoides* adults show also differences in calyx area across depth environments, with mesophotic corals having smaller calyxes compared to their shallow conspecifics, similarly to other depth-generalist coral species (Malik et al., 2020; Studivan et al., 2019). Indeed, the size and spacing of calyxes can be plastic in response to changing light conditions at depth, acting to focus, redirect, or dissipate light to enhance light harvesting or reflectance (Nir et al., 2011; Ow and Todd, 2010; Rocha et al., 2014). Additionally, having larger calyxes increases drag, which could increase retention of pray in high water flow environments such as shallow reefs (Dustan, 1975).

Morphological changes between shallow and mesophotic conspecifics have also been attributed to different calcification rates (Lesser et al., 2010; Malik et al., 2020; Risk and Sammarco, 1991), which have

been shown to significantly decline along the light gradient (Lesser et al., 2010; Mass et al., 2007). In the present study, we observed an analogous mineral distribution between shallow and mesophotic P. astreoides adults (Fig. 2), suggesting that, even in the case of lower calcification rates in deeper water, the bulk skeletal growth dynamics are highly similar. Little information exists on the calcification rates of P. astreoides below 30 m depth. In the Puerto Rican shelf, the calcification rate of this species does not show a clear relationship with depth going from shallow to mesophotic reefs (6-47 m)(Groves et al., 2018). All these results suggest that light might not be the primary factor controlling growth for this species, or that *P. astreoides* is able to adjust its biomineralization machinery to changing light regimes across wide depth ranges. Such capability of maintaining homogeneous skeleton development dynamics across depths could significantly facilitate the successful growth of early P. astreoides life stages migrating across the vertical gradient, increasing connectivity between reefs.

Response of populations to local environmental features can be either due to evolutionary changes underlined by genetic differentiation

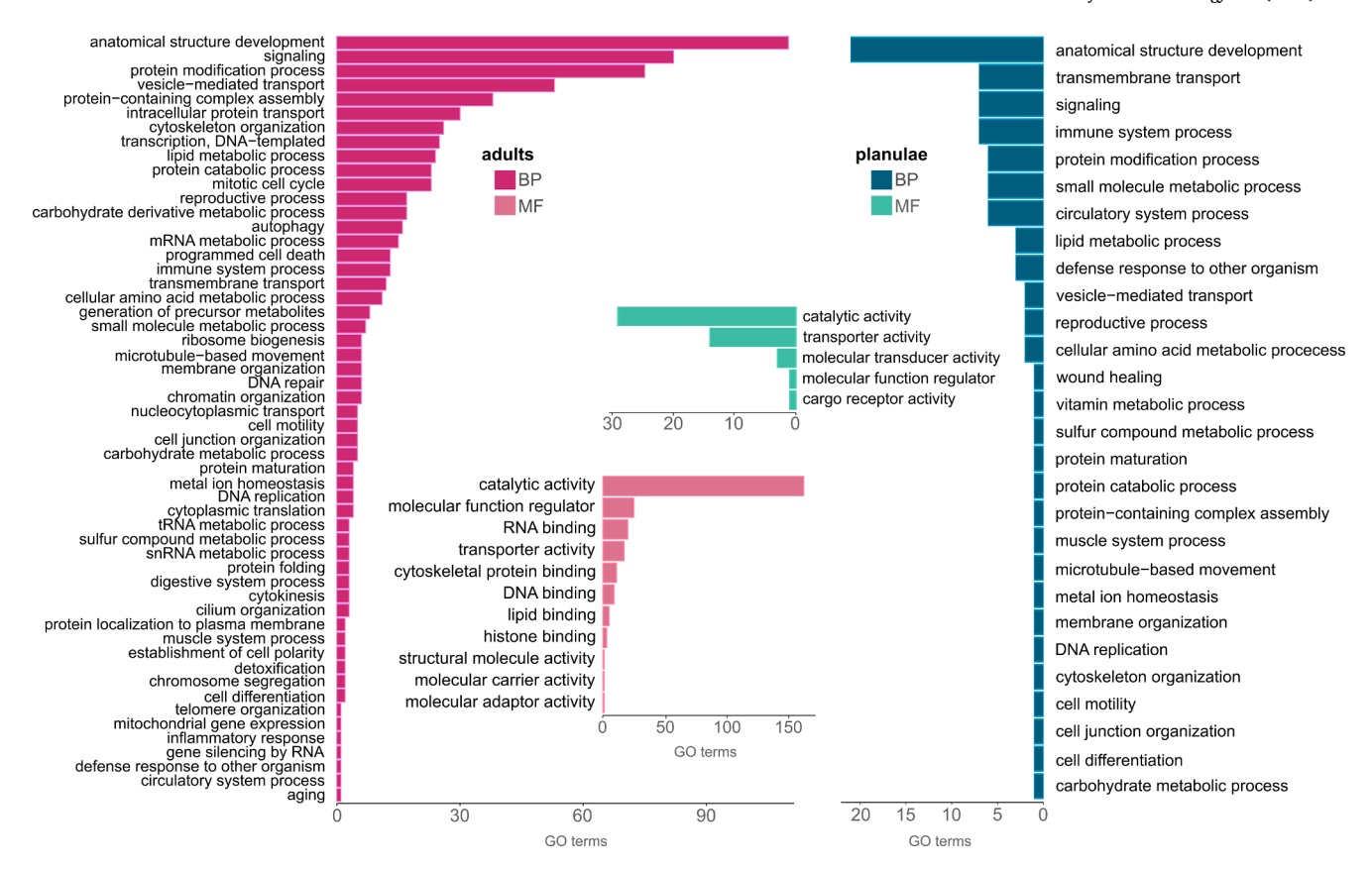


Fig. 6. Gene ontology enrichment analysis of DEGs in mesophotic versus shallow corals. Dendrogram on the left showing enriched Gene Ontology (GO) terms clustered according to the portion of identical genes shared. The dot plot shows by color the up-regulated (positive adjusted p value) or down-regulated (negative adjusted p value) DEGs per each GO term detected, respectively, in the mesophotic versus shallow adult comparison (left side of the dot plot) and in the mesophotic versus shallow planulae comparison (right side of the dot plot). The size of the dots depicts the number of genes found to be significantly differentially expressed within each term

among populations (Sanford and Kelly, 2011; Savolainen et al., 2013), or can be driven by mechanisms enabling phenotypic plasticity of the species (Thibert-Plante and Hendry, 2011). Genetic connectivity between shallow and mesophotic P. astreoides adults (Fig. 3a) does not lend support to selection for genetic adaptation to differing environments across depths. Instead, it suggests that it is the *P. astreoides* phenotypic plasticity that primarily determines the species persistence across the broad vertical cline in Bermuda. It must be noted, however, that these suppositions are based on a restricted sample size, attributable to the strong limitations on sampling corals from protected environments. This limits accurate estimation of genetic differentiation between shallow and mesophotic populations. Still, there is large variability in sample size employed in population genomic work, suggesting that there is no agreed-on universal sample size rule to precisely characterize genetic variation across populations and taxa (reviewed in Phillips et al., 2019). It appears, however, that even with restricted sample sizes (<10) it is possible to adequately estimate differentiation between populations (Hoban et al., 2013; Nazareno et al., 2017; Phillips et al., 2019; Qu et al., 2020; Trask et al., 2011; Willing et al., 2012), particularly in the case of populations that have confined geographical distributions (Phillips et al., 2019), such as corals in Bermuda. In addition, several studies have shown that increasing the sample size only minorly improves, or does not improve at all, preciseness of the genetic diversity estimation (Hoban et al., 2013; Kumasaka et al., 2010; Qu et al., 2020; Zeggini et al., 2005). Furthermore, screening a large number of SNPs (>1,500), as in this study, can compensate for the small sample size and produce accurate assessment of genetic differentiation (Jeffries et al., 2016; Nazareno et al., 2017; Ou et al., 2020; Zimmerman et al., 2020). Nevertheless, further studies using a larger sample size are needed to accurately assess the degree of genetic connectivity between shallow

and mesophotic P. astreoides corals in Bermuda.

The observed pattern of genetic similarity, which involves a broader depth range than previously shown for this species in Bermuda (Serrano et al., 2016), is reflected by the degree of variation between the transcriptome profiles of shallow and mesophotic corals. In fact, while wide gene expression changes (>4000 DEGs, 15%-39% of the total expressed genes) were found between mesophotic and shallow *S. pistillata* corals shown to be genetically differentiated (Malik et al., 2020; Scucchia et al., 2021), a much lower degree of change was found here between mesophotic and shallow *P. astreoides* adults (1.8% of the total expressed genes, Fig. 4c). These results are comparable to the 3.6% of total expressed genes that were found to be differentially expressed between depths and across several sites in the Gulf of Mexico and Belize for *M. cavernosa* corals (Studivan and Voss, 2020), which had been shown to be genetically connected (Studivan and Voss, 2018).

For other coral species in Bermuda, genetic differentiation has been observed across the vertical gradient and has been attributed to the different coral reproductive modes (Bongaerts et al., 2017). Divergence by depth is thought to be prevalent in species with a brooding reproductive mode compared to broadcast spawners (Bongaerts et al., 2010; Gorospe and Karl, 2015; Van Oppen et al., 2011). With its brooding reproductive mode and a short pelagic larval duration, *P. astreoides* would be expected to have low levels of gene flow. However, divergence by depth has been observed in both broadcasting and brooding coral species (Bongaerts et al., 2010; Brazeau et al., 2013; Serrano et al., 2014, 2016; Van Oppen et al., 2011), suggesting that other location-specific extrinsic processes contribute in determining vertical connectivity (Serrano et al., 2016), such as selection, temporal shifts in population dynamics and sweepstakes reproductive success (Eldon et al., 2016). The presence of genetic connectivity among *P. astreoides* populations in

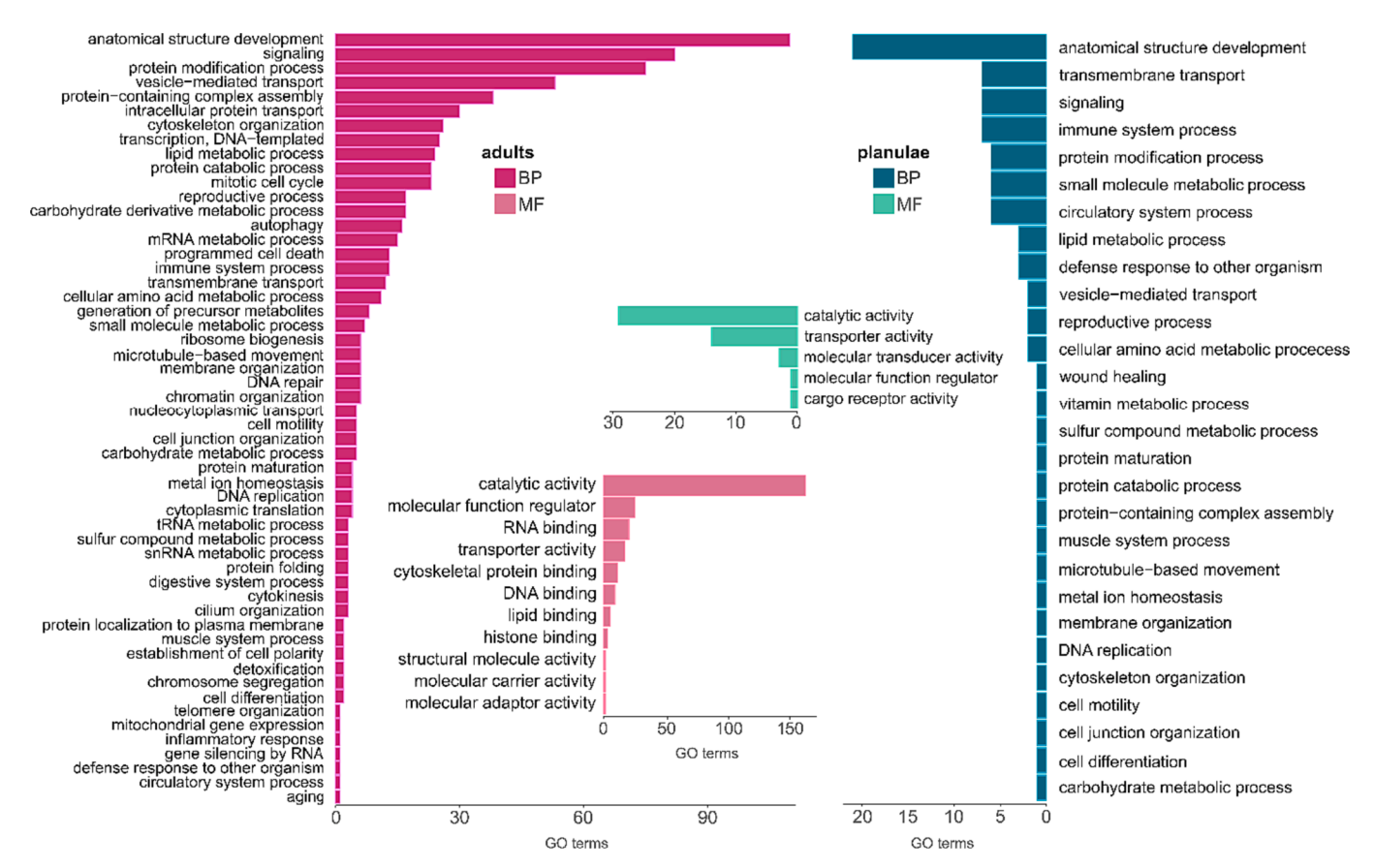


**Fig. 7. Gene ontology slim terms enrichment analysis of selected WGCNA clusters.** Significantly enriched GOslim categories are arranged in the biological process (BP) and the molecular function (MF) categories for both the within adults (pink) and within planulae (green) comparisons. GO enrichment analysis was performed on the modules clusters with the largest significant differences in mean eigengene expression (p < 0.001) between corals at different depth environments for both the within adults and within planulae comparison (cluster 5 for the adults and 7 for the planulae, Fig. 5). The x axis indicates the total number of enriched GO terms associated to each GOslim category. (For interpretation of the references to color in this figure legend, the reader is referred to the web version of this article.)

Bermuda would suggest substantial levels of historic or contemporary larval migration between shallow and mesophotic reefs, which may be attributed to the Bermuda vertical mixing patterns (Reich et al., 2017). Such consideration finds support in the fact that planulae of *P. astreoides* from the same shallow and mesophotic reefs sites of this study exhibited the capacity to survive and settle under reciprocal light conditions (Goodbody-Gringley et al., 2021).

Altering the expression of genes is one mechanism allowing organisms to adjust to environmental variance. Compared to the adults, P. astreoides planulae showed a higher degree of variation of transcriptome profiles between shallow and mesophotic individuals (8.9% of total expressed genes are differentially expressed). Such larger changes compared to the adult phase are likely related to broad cell differentiation processes occurring at invertebrate larval stages (Arenas-Mena, 2010) which dramatically alter a cell's shape, size and energy requirements (Ng et al., 2019). This is also indicated by the enrichment of biological functions related to cell differentiation and to membrane and cytoskeleton organization observed in mesophotic and shallow planulae (Fig. 7). Cellular processes, including differentiation, are sensitive to both mechanical and chemical stimuli from the environment (Ng et al., 2019). In marine habitats, environmental signals and features, particularly light, greatly change from shallow to mesophotic reefs, determining a change in the energy available to the symbionts and coral host for the maintenance of cellular processes and for organismal growth. Several functions related to energy metabolism (i.e., lipid metabolic process, carbohydrate metabolic process) as well as functions related to organism growth (i.e., anatomical structure development) showed an opposite module-trait correlation in mesophotic and shallow corals at

both adults and planulae stages (Fig. 7), suggesting a differential utilization of energy for organismal growth across the depth gradient.

Energy acquisition in organisms is regulated at the cellular level by a variety of enzymes, including peptidases (Wilson et al., 2013). Genes related to peptidases activity are up-regulated in mesophotic corals across developmental stages (Fig. 6), providing further indication that energy metabolism is differentially regulated across the depth gradient. Peptidases are also involved in a variety of other cellular processes such as growth, cell-cell interactions, differentiation and play crucial roles in the regulation of immune functions (Lendeckel et al., 2002). Immune system processes appear to have a depth-dependent pattern across developmental stages, being up-regulated in shallow corals compared to their mesophotic counterparts (Figs. 6 and 7). This suggests higher levels of pathogen invasion or disease in the shallow environment compared to deeper depths, although coral diseases have been recorded in mesophotic environments (Bongaerts et al., 2010; Calnan et al., 2007) and for some coral species they appear to be spread over the entire depth gradient (Morais and Santos, 2022).

In corals exposed to temperature stress some immunity functions are enhanced (Mydlarz et al., 2010), such as in the case of corals living in shallow environments, that are characterized by wider temperature fluctuations compared to mesophotic ones (Hinderstein et al., 2010). Another hallmark of the environmental stress response is the regulation of genes linked to ribosome biogenesis (Sáez-Vásquez and Delseny, 2019), which are up-regulated in shallow *P. astreoides* adults compared to their mesophotic conspecifics (Fig. 7). Such patterns reveal a potential genomic mechanism employed by this species to colonize and persist in the thermally variable shallow environment. In fact, plasticity of gene

expression involved in environmental stress response correlates with lower susceptibility to summer bleaching events in *P. astreoides* adults inhabiting shallow reef locations (Kenkel and Matz, 2017).

The similar regulation of stress response genes among shallow planulae, collected right after release, and adults observed here suggests that a legacy of environmentally induced effects in parents can be carried over to their offspring. Parental thermal history, in fact, often affects the thermal tolerance of the progeny in many marine invertebrates, improving performance under thermal stress through, for example, epigenetic effects (reviewed in Byrne et al., 2020). Whilst acclimatization through epigenetics in reef building corals has received substantial attention (Putnam, 2021), nothing is yet known about potential epigenetic mechanisms linked to the persistence of corals across wide depth ranges, thus constituting a fertile field of investigation.

The ability of P. astreoides planulae to colonize highly different light environments may stem from the endosymbionts photosynthetic plasticity. Shallow and mesophotic P. astreoides corals in fact host a similar consortium of Symbiodinium species (Fig. 3b), revealing minimal symbiont depth-zonation at these sites in Bermuda. Such low differentiation in symbiont consortia may reflect Bermuda isolated high-latitudinal location and the less steep environmental gradients compared with other regions in the Caribbean, which may also explain the level of coral genetic connectivity (Gould et al., 2021; Reich et al., 2017; Serrano et al., 2014). Commonly, the association with different symbiont types across depths is considered a trait of depth generalist corals to broaden their vertical distribution range (Bongaerts et al., 2010). Symbiont types can in fact differ in photosynthetic pigments quality and quantity, which determine different photo-physiological efficiencies at depth (Frade et al., 2008). However, depth stratification of the algal symbiont is not a universal trend, as demonstrated here for P. astreoides and by previous investigations for other coral species (Bongaerts et al., 2013; Chan et al., 2009; Martinez et al., 2021; Studivan and Voss, 2020; Ziegler et al., 2015). The same symbiont type can in fact employ different photoacclimatory strategies to adjust to differing light conditions at depth, by for example reorganizing the photosynthetic machinery to cope with different light intensities (Lesser et al., 2010; Ziegler et al., 2015). The symbiont genus Symbiodinium (formerly clade A, LaJeunesse et al., 2018) has been shown to possess high resistance to light variations compared to other genera, promoting survival of the host at high light intensities and conferring resistance to bleaching (Reynolds et al., 2008). These photo-physiological characteristics of the Symbiodinium genus may enhance the capacity of *P. astreoides* planulae to successfully migrate along the vertical gradient.

Overall, our investigation has identified key morphological and genetic mechanisms underlying the plasticity of P. astreoides planulae and adults that enable them to survive along broad depth gradients. Several aspects contribute to this capacity, including micro-skeletal features that may optimize symbiont light capture in the diverse light-environments, differential regulation of metabolism-related functions suggesting a differential utilization of energy across the depth gradient, and differential regulation of immune system and ribosome biogenesis processes to cope with environmental stress, particularly in the shallow environment. These variations in micro-skeletal morphology and gene expression patterns across depth zones do not appear to limit coral connectivity. Rather, the low genetic differentiation, analogous bulk skeletal growth dynamics and the uniform consortium of Symbiodinium species indicate that the micro-skeletal and gene expression differences observed between shallow and depth zones stem from plasticity of this species in adjusting to different environmental conditions at depths. While cautioning that these results should be viewed with the caveat of a restricted sample size, we emphasize that the combination of multiple techniques and the overall correspondence of processes across different assays demonstrates the robust nature of our work.

It must be noted that the pattern of connectivity across depths observed here may derive from a dominant one-way flux of coral planulae, considering that several studies presented genetic evidence of asymmetric (only from shallow to deep) gene flow across the depth gradient (Bongaerts et al., 2017; Prada and Hellberg, 2013; Serrano et al., 2014; Shlesinger and Loya, 2021). An ex-situ experiment showed that mesophotic P. astreoides planulae have a greater dispersal potential and the ability to survive and settle under shallow light conditions (Goodbody-Gringley et al., 2021), suggesting that for this species in Bermuda larval dispersal may preferentially occur up the slope (from deep to shallow). However, for that study the only environmental factor manipulated to mimic shallow and mesophotic conditions was light intensity, leaving unaddressed the influence on larval dispersal and settlement of other depth-related factors (i.e., temperature, water flow, food availability, sedimentation, herbivory). Thus, it still remains unclear if mesophotic population of P. astreoides in Bermuda act as larval sink or source, or both, for their shallow-water conspecifics. It should also be underlined that such refugia capacity may only be limited to P. astreoides at this specific location. In fact, previous work has shown that other coral species lack refugia potential (Bongaerts et al., 2017), which also appears to be location-specific (Bongaerts et al., 2017; Serrano et al., 2016). Thus, the reseeding and buffer capacity of mesophotic reefs may not be considered as a global trend. A deeper understanding of coral acclimatory capability and of genetic connectivity among coral populations is crucial in the context of global environmental change, as it enables to assess coral population dynamics and future potential shifts in reef ecosystems structure and function. As such, future research priorities should include in situ reciprocal transplantation experiments using planulae and adults to assess bidirectional plasticity across shallow and mesophotic environments for multiple corals species in Bermuda and other un-assessed locations.

#### **Author contributions**

G.G.G and T.M. designed the experiment and conducted the field-work in Bermuda. F.S., K.W. and H.P. conducted the molecular analyses. F.S., P.Z. and T.M. conducted the skeletal analysis. F.S. analyzed the data and wrote the manuscript. All authors contributed to the editing and refinement of the final manuscript.

# CRediT authorship contribution statement

Federica Scucchia: Formal analysis, Investigation, Visualization, Writing – original draft, Writing – review & editing. Kevin Wong: Formal analysis, Writing – review & editing. Paul Zaslansky: Investigation, Supervision, Writing – review & editing. Hollie M. Putnam: Funding acquisition, Project administration, Writing – review & editing. Gretchen Goodbody-Gringley: Conceptualization, Funding acquisition, Project administration, Writing – review & editing. Tali Mass: Conceptualization, Funding acquisition, Investigation, Project administration, Supervision, Writing – review & editing.

#### **Declaration of Competing Interest**

The authors declare that they have no known competing financial interests or personal relationships that could have appeared to influence the work reported in this paper.

# Data availability

The links to all data/code have been included in the paper.

# Acknowledgments

We thank Alex Chequer, Hagai Nativ, Shai Einbinder and Stephane Martinez for their help in collecting corals from the wild and their fieldwork assistance in Bermuda. We also thank Margaret Schedl for her help with the molecular samples, the HZB for granting us the use of the BAMline and the BAMline team member Michael Sintschuk for

assistance with making it possible to image the corals.

#### Funding

This project received funding from the United States National Science Foundation (NSF #1937770 to GGG), the United States – Israel Binational Science Foundation (BSF #2019653 to TM and BSF #2016321 to HMP and TM) and a Grant-in-Aid award from the Bermuda Institute of Ocean Sciences.

#### Code availability

All the scripts employed to analyze the RNA- seq data are accessible through the electronic notebook https://github.com/fscucchia/Pastre oides development depth.

### Appendix A. Supplementary data

Supplementary data to this article can be found online at  $\frac{\text{https:}}{\text{doi.}}$  org/10.1016/j.jsb.2023.108036.

#### References

- Appeldoorn, R., Ballantine, D., Bejarano, I., Carlo, M., Nemeth, M., Otero, E., Pagan, F., Ruiz, H., Schizas, N., Sherman, C., Weil, E., 2016. Mesophotic coral ecosystems under anthropogenic stress: a case study at Ponce, Puerto Rico. Coral Reefs 35, 63–75. https://doi.org/10.1007/s00338-015-1360-5.
- Arenas-Mena, C., 2010. Indirect development, transdifferentiation and the macroregulatory evolution of metazoans. Phil. Trans. R. Soc. B 365, 653–669. https://doi.org/10.1098/rstb.2009.0253.
- Ashburner, M., Ball, C.A., Blake, J.A., Botstein, D., Butler, H., Cherry, J.M., Davis, A.P., Dolinski, K., Dwight, S.S., Eppig, J.T., Harris, M.A., Hill, D.P., Issel-Tarver, L., Kasarskis, A., Lewis, S., Matese, J.C., Richardson, J.E., Ringwald, M., Rubin, G.M., Sherlock, G., 2000. Gene Ontology: tool for the unification of biology. Nat. Genet. 25, 25–29. https://doi.org/10.1038/75556.
- Auwera, G.A., Carneiro, M.O., Hartl, C., Poplin, R., del Angel, G., Levy-Moonshine, A., Jordan, T., Shakir, K., Roazen, D., Thibault, J., Banks, E., Garimella, K.V., Altshuler, D., Gabriel, S., DePristo, M.A., 2013. From FastQ Data to High-Confidence Variant Calls: The Genome Analysis Toolkit Best Practices Pipeline. Curr. Protoc. Bioinformatics 43. https://doi.org/10.1002/0471250953.bi1110s43.
- Bolger, A.M., Lohse, M., Usadel, B., 2014. Trimmomatic: a flexible trimmer for Illumina sequence data. Bioinformatics 30, 2114–2120. Doi: 10.1093/bioinformatics/btu170.
- Bongaerts, Pim, Riginos, C., Ridgway, T., Sampayo, E.M., van Oppen, M.J.H., Englebert, N., Vermeulen, F., Hoegh-Guldberg, O., 2010. Genetic Divergence across Habitats in the Widespread Coral Seriatopora hystrix and Its Associated Symbiodinium. PLoS ONE 5, e10871. Doi: 10.1371/journal.pone.0010871.
- Bongaerts, P., Ridgway, T., Sampayo, E.M., Hoegh-Guldberg, O., 2010a. Assessing the 'deep reef refugia' hypothesis: focus on Caribbean reefs. Coral Reefs 29, 309–327. https://doi.org/10.1007/s00338-009-0581-x.
- Bongaerts, P., Sampayo, E., Bridge, T., Ridgway, T., Vermeulen, F., Englebert, N., Webster, J., Hoegh-Guldberg, O., 2011. Symbiodinium diversity in mesophotic coral communities on the Great Barrier Reef: a first assessment. Mar. Ecol. Prog. Ser. 439, 117–126. https://doi.org/10.3354/meps09315.
- Bongaerts, P., Frade, P.R., Ogier, J.J., Hay, K.B., van Bleijswijk, J., Englebert, N., Vermeij, M.J., Bak, R.P., Visser, P.M., Hoegh-Guldberg, O., 2013a. Sharing the slope: depth partitioning of agariciid corals and associated Symbiodinium across shallow and mesophotic habitats (2–60 m) on a Caribbean reef. BMC Evol. Biol. 13, 205. https://doi.org/10.1186/1471-2148-13-205.
- Bongaerts, P., Muir, P., Englebert, N., Bridge, T.C.L., Hoegh-Guldberg, O., 2013b. Cyclone damage at mesophotic depths on Myrmidon Reef (GBR). Coral Reefs 32, 935. https://doi.org/10.1007/s00338-013-1052-y.
- Bongaerts, P., Carmichael, M., Hay, K.B., Tonk, L., Frade, P.R., Hoegh-Guldberg, O., 2015. Prevalent endosymbiont zonation shapes the depth distributions of scleractinian coral species. R. Soc. Open Sci. 2 (2), 140297.
- Bongaerts, P., Riginos, C., Brunner, R., Englebert, N., Smith, S.R., Hoegh-Guldberg, O., 2017. Deep reefs are not universal refuges: Reseeding potential varies among coral species. Sci. Adv. 3, e1602373.
- Brazeau, D.A., Lesser, M.P., Slattery, M., 2013. Genetic Structure in the Coral, Montastraea cavernosa: Assessing Genetic Differentiation among and within Mesophotic Reefs. PLoS ONE 8, e65845. Doi: 10.1371/journal.pone.0065845.
- Buchfink, B., Xie, C., Huson, D.H., 2015. Fast and sensitive protein alignment using DIAMOND. Nat. Methods 12, 59–60. https://doi.org/10.1038/nmeth.3176.
- Byrne, M., Foo, S.A., Ross, P.M., Putnam, H.M., 2020. Limitations of cross- and multigenerational plasticity for marine invertebrates faced with global climate change. Glob. Chang. Biol. 26, 80–102. https://doi.org/10.1111/gcb.14882.
- Calnan, J.M., Smith, T.B., Nemeth, R.S., Kadison, E., Blondeau, J., 2007. Coral disease prevalence and host susceptibility on mid-depth and deep reefs in the United States Virgin Islands. RBT 56. https://doi.org/10.15517/rbt.v56i0.5589.

- Carpenter, G.E., Chequer, A.D., Weber, S., Mass, T., Goodbody-Gringley, G., 2022. Light and photoacclimatization drive distinct differences between shallow and mesophotic coral communities. Ecosphere 13. https://doi.org/10.1002/ecs2.4200.
- Chan, Y.L., Pochon, X., Fisher, M.A., Wagner, D., Concepcion, G.T., Kahng, S.E., Toonen, R.J., Gates, R.D., 2009. Generalist dinoflagellate endosymbionts and host genotype diversity detected from mesophotic (67–100 m depths) coral Leptoseris. BMC Ecol. 9, 21. https://doi.org/10.1186/1472-6785-9-21.
- Cramer, K.L., Donovan, M.K., Jackson, J.B.C., Greenstein, B.J., Korpanty, C.A., Cook, G. M., Pandolfi, J.M., 2021. The transformation of Caribbean coral communities since humans. Ecol. Evol. 11, 10098–10118. https://doi.org/10.1002/ece3.7808.
- de Putron, S.J., Smith, S.R., 2011. Planula release and reproductive seasonality of the scleractinian coral Porites astreoides in Bermuda, a high-latitude reef. Bull. Mar. Sci. 87, 75–90. https://doi.org/10.5343/bms.2009.1027.
- Dustan, P., 1975. Growth and form in the reef-building coral Montastrea annularis. Mar. Biol. 33, 101–107. https://doi.org/10.1007/BF00390714.
- Einbinder, S., Gruber, D.F., Salomon, E., Liran, O., Keren, N., Tchernov, D., 2016. Novel Adaptive Photosynthetic Characteristics of Mesophotic Symbiotic Microalgae within the Reef-Building Coral, Stylophora pistillata. Front. Mar. Sci. 3 https://doi.org/ 10.3389/fmars.2016.00195.
- Eldon, B., Riquet, F., Yearsley, J., Jollivet, D., Broquet, T., 2016. Current hypotheses to explain genetic chaos under the sea. Curr. Zool. 62, 551–566. https://doi.org/ 10.1093/cz/zow094.
- Enríquez, S., Méndez, E.R., Prieto, R.I., 2005. Multiple scattering on coral skeletons enhances light absorption by symbiotic algae. Limnol. Oceanogr. 50, 1025–1032. https://doi.org/10.4319/10.2005.50.4.1025.
- Falkowski, P.G., Dubinsky, Z., Muscatine, L., Porter, J.W., 1984. Light and the Bioenergetics of a Symbiotic Coral. Bioscience 34, 705–709. https://doi.org/ 10.2307/1309663.
- Frade, P.R., Bongaerts, P., Winkelhagen, A.J.S., Tonk, L., Bak, R.P.M., 2008. In situ photobiology of corals over large depth ranges: A multivariate analysis on the roles of environment, host, and algal symbiont. Limnol. Oceanogr. 53, 2711–2723. https://doi.org/10.4319/lo.2008.53.6.2711.
- Fricke, H., Meischner, D., 1985. Depth limits of Bermudan scleractinian corals: a submersible survey. Mar. Biol. 88, 175–187. https://doi.org/10.1007/BF00397165.
- Goodbody-Gringley, G., Noyes, T., Smith, S.R., Loya, Y., Puglise, K.A., Bridge, T.C.L.,
  2019. Bermuda. In: Loya, Y., Puglise, K.A., Bridge, T.C.L. (Eds.), Mesophotic coral ecosystems. Springer, Berlin, Germany, pp. 31–45.
  Goodbody-Gringley, G., Scucchia, F., Ju, R., Chequer, A., Einbinder, S., Martinez, S.,
- Goodbody-Gringley, G., Scucchia, F., Ju, R., Chequer, A., Einbinder, S., Martinez, S., Nativ, H., Mass, T., 2021. Plasticity of Porites astreoides Early Life History Stages Suggests Mesophotic Coral Ecosystems Act as Refugia in Bermuda. Front. Mar. Sci. 8, 702672 https://doi.org/10.3389/fmars.2021.702672.
- Goodbody-Gringley, G., Waletich, J., 2018. Morphological Plasticity of the Depth Generalist Coral, Montastraea Cavernosa, on Mesophotic Reefs in Bermuda. Ecology 99 (7). 1688–1690.
- Goodbody-Gringley, G., Wong, K.H., Becker, D.M., Glennon, K., de Putron, S.J., 2018. Reproductive ecology and early life history traits of the brooding coral, Porites astreoides, from shallow to mesophotic zones. Coral Reefs 37, 483–494. https://doi. org/10.1007/s00338-018-1673-2
- Görner, W., Hentschel, M.P., Müller, B.R., Riesemeier, H., Krumrey, M., Ulm, G., Diete, W., Klein, U., Frahm, R., 2001. BAMline: the first hard X-ray beamline at BESSY II. Nucl. Instrum. Methods Phys. Res., Sect. A 467–468, 703–706. https://doi.org/10.1016/S0168-9002(01)00466-1.
- Gorospe, K.D., Karl, S.A., 2015. Depth as an Organizing Force in Pocillopora damicornis: Intra-Reef Genetic Architecture. PLoS ONE 10, e0122127. Doi: 10.1371/journal.pon 201201277
- Gould, K., Bruno, J.F., Ju, R., Goodbody-Gringley, G., 2021. Upper-mesophotic and shallow reef corals exhibit similar thermal tolerance, sensitivity and optima. Coral Reefs 40, 907–920. https://doi.org/10.1007/s00338-021-02095-w.
- Groves, S.H., Holstein, D.M., Enochs, İ.C., Kolodzeij, G., Manzello, D.P., Brandt, M.E., Smith, T.B., 2018. Growth rates of Porites astreoides and Orbicella franksi in mesophotic habitats surrounding St. Thomas, US Virgin Islands. Coral Reefs 37, 345–354. https://doi.org/10.1007/s00338-018-1660-7.
- Hinderstein, L.M., Marr, J.C.A., Martinez, F.A., Dowgiallo, M.J., Puglise, K.A., Pyle, R.L., Zawada, D.G., Appeldoorn, R., 2010. Theme section on "Mesophotic Coral Ecosystems: Characterization, Ecology, and Management". Coral Reefs 29, 247–251. https://doi.org/10.1007/s00338-010-0614-5.
- Hoban, S., Gaggiotti, O., Bertorelle, G., O'Hara, R.B., 2013. Sample Planning Optimization Tool for conservation and population Genetics (SPOTG): a software for choosing the appropriate number of markers and samples. Methods Ecol. Evol. 4 (3), 299–303.
- Iglesias-Prieto, R., Beltrán, V.H., LaJeunesse, T.C., Reyes-Bonilla, H., Thomé, P.E., 2004. Different algal symbionts explain the vertical distribution of dominant reef corals in the eastern Pacific. Proc. R. Soc. Lond. B 271, 1757–1763. https://doi.org/10.1098/ rspb. 2004. 2757
- Jeffries, D.L., Copp, G.H., Lawson Handley, L., Olsén, K.H., Sayer, C.D., Hänfling, B., 2016. Comparing RADseq and microsatellites to infer complex phylogeographic patterns, an empirical perspective in the Crucian carp, Carassius carassius, L. Mol. Ecol. 25, 2997–3018. https://doi.org/10.1111/mec.13613.
- Kenkel, C.D., Matz, M.V., 2017. Gene expression plasticity as a mechanism of coral adaptation to a variable environment. Nat. Ecol. Evol. 1, 0014. https://doi.org/ 10.1028/c41550.016.0014
- Kim, D., Paggi, J.M., Park, C., Bennett, C., Salzberg, S.L., 2019. Graph-based genome alignment and genotyping with HISAT2 and HISAT-genotype. Nat. Biotechnol. 37, 907–915. https://doi.org/10.1038/s41587-019-0201-4.
- Kramer, N., Guan, J., Chen, S., Wangpraseurt, D., Loya, Y., 2022a. Morpho-functional traits of the coral Stylophora pistillata enhance light capture for photosynthesis at

- mesophotic depths. Commun Biol 5, 861. https://doi.org/10.1038/s42003-022-03820.4
- Kramer, N., Tamir, R., Ben-Zvi, O., Jacques, S.L., Loya, Y., Wangpraseurt, D., 2022b. Efficient light-harvesting of mesophotic corals is facilitated by coral optical traits. Funct. Ecol. 36, 406–418. https://doi.org/10.1111/1365-2435.13948.
- Kumasaka, N., Yamaguchi-Kabata, Y., Takahashi, A., Kubo, M., Nakamura, Y., Kamatani, N., 2010. Establishment of a standardized system to perform population structure analyses with limited sample size or with different sets of SNP genotypes. J. Hum. Genet. 55, 525–533. https://doi.org/10.1038/jhg.2010.63.
- LaJeunesse, T.C., Parkinson, J.E., Gabrielson, P.W., Jeong, H.J., Reimer, J.D., Voolstra, C.R., Santos, S.R., 2018. Systematic Revision of Symbiodiniaceae Highlights the Antiquity and Diversity of Coral Endosymbionts. Curr. Biol. 28, 2570–2580.e6. https://doi.org/10.1016/j.cub.2018.07.008.
- Langfelder, P., Horvath, S., 2008. WGCNA: an R package for weighted correlation network analysis. BMC Bioinf. 9, 559. https://doi.org/10.1186/1471-2105-9-559.
  Lendeckel, U., Kähne, T., Riemann, D., Neubert, K., Arndt, M., Reinhold, D., 2002. In:
- Lendeckel, U., Kanne, I., Kiemann, D., Neuberr, K., Arnat, M., Reinnold, D., 2002. In Advances in Experimental Medicine and BiologyCellular Peptidases in Immune Functions and Diseases 2. Kluwer Academic Publishers, Boston, pp. 1–24.
- Lesser, M.P., Slattery, M., Leichter, J.J., 2009. Ecology of mesophotic coral reefs. J. Exp. Mar. Biol. Ecol. 375, 1–8. https://doi.org/10.1016/j.jembe.2009.05.009.
- Lesser, M.P., Slattery, M., Stat, M., Ojimi, M., Gates, R.D., Grottoli, A., 2010.

  Photoacclimatization by the coral Montastraea cavernosa in the mesophotic zone: light, food, and genetics. Ecology 91, 990–1003. https://doi.org/10.1890/09-03131
- Lesser, M.P., Slattery, M., Mobley, C.D., 2018. Biodiversity and Functional Ecology of Mesophotic Coral Reefs. Annu. Rev. Ecol. Evol. Syst. 49, 49–71. https://doi.org/ 10.1146/annurev-ecolsys-110617-062423.
- Love, M., Anders, S., Huber, W., 2013. Differential analysis of RNA-Seq data at the gene level using the DESeq2 package. Heidelberg: European Molecular Biology Laboratory (EMBL).
- Love, M.I., Huber, W., Anders, S., 2014. Moderated estimation of fold change and dispersion for RNA-seq data with DESeq2. Genome Biol. 15, 550. https://doi.org/ 10.1186/s13059-014-0550-8.
- Makovetsky, R., Piche, N., Marsh, M., 2018. Dragonfly as a Platform for Easy Image-based Deep Learning Applications. Microsc. Microanal. 24, 532–533. https://doi.org/10.1017/S143192761800315X.
- Malik, A., Einbinder, S., Martinez, S., Tchernov, D., Haviv, S., Almuly, R., Zaslansky, P., Polishchuk, I., Pokroy, B., Stolarski, J., Mass, T., 2020. Molecular and skeletal fingerprints of scleractinian coral biomineralization: From the sea surface to mesophotic depths. Acta Biomater. 120. 263–276.
- Martin, M., 2011. Cutadapt removes adapter sequences from high-throughput sequencing reads. EMBnet j. 17, 10. https://doi.org/10.14806/ej.17.1.200.
- Martinez, S., Kolodny, Y., Shemesh, E., Scucchia, F., Nevo, R., Levin-Zaidman, S., Paltiel, Y., Keren, N., Tchernov, D., Mass, T., 2020. Energy Sources of the Depth-Generalist Mixotrophic Coral Stylophora pistillata. Front. Mar. Sci. 7, 566663 https://doi.org/10.3389/fmars.2020.566663.
- Martinez, S., Bellworthy, J., Ferrier-Pagès, C., Mass, T., 2021. Selection of mesophotic habitats by Oculina patagonica in the Eastern Mediterranean Sea following global warming. Sci. Rep. 11, 18134. https://doi.org/10.1038/s41598-021-97447-5
- warming. Sci. Rep. 11, 18134. https://doi.org/10.1038/s41598-021-97447-5.

  Mass, T., Einbinder, S., Brokovich, E., Shashar, N., Vago, R., Erez, J., Dubinsky, Z., 2007.

  Photoacclimation of Stylophora pistillata to light extremes: metabolism and calcification. Mar. Ecol. Prog. Ser. 334, 93–102. https://doi.org/10.3354/meps334093.
- McKenna, A., Hanna, M., Banks, E., Sivachenko, A., Cibulskis, K., Kernytsky, A., Garimella, K., Altshuler, D., Gabriel, S., Daly, M., DePristo, M.A., 2010. The Genome Analysis Toolkit: A MapReduce framework for analyzing next-generation DNA sequencing data. Genome Res. 20, 1297–1303. https://doi.org/10.1101/gr.107524.110.
- Morais, J., Santos, B.A., 2022. Prevalence and extent of coral diseases in shallow and mesophotic reefs of the Southwestern Atlantic. Coral Reefs 41 (5), 1317–1322.
- Mydlarz, L.D., McGinty, E.S., Harvell, C.D., 2010. What are the physiological and immunological responses of coral to climate warming and disease? J. Exp. Biol. 213, 934–945. https://doi.org/10.1242/jeb.037580.
- Nazareno, A.G., Bemmels, J.B., Dick, C.W., Lohmann, L.G., 2017. Minimum sample sizes for population genomics: an empirical study from an Amazonian plant species. Mol. Ecol. Resour. 17, 1136–1147. https://doi.org/10.1111/1755-0998.12654.
- Ng, I.C., Pawijit, P., Tan, J., Yu, H., 2019. In: Encyclopedia of Biomedical Engineering. Elsevier, pp. 225–236.
- Nir, O., Gruber, D.F., Einbinder, S., Kark, S., Tchernov, D., 2011. Changes in scleractinian coral Seriatopora hystrix morphology and its endocellular Symbiodinium characteristics along a bathymetric gradient from shallow to mesophotic reef. Coral Reefs 30, 1089–1100. https://doi.org/10.1007/s00338-011-0801-z.
- Ow, Y.X., Todd, P.A., 2010. Light-induced morphological plasticity in the scleractinian coral Goniastrea pectinata and its functional significance. Coral Reefs 29, 797–808. https://doi.org/10.1007/s00338-010-0631-4.
- Pandolfi, J.M., Connolly, S.R., Marshall, D.J., Cohen, A.L., 2011. Projecting Coral Reef Futures Under Global Warming and Ocean Acidification. Science 333, 418–422. https://doi.org/10.1126/science.1204794.
- Pérez-Rosales, G., Rouzé, H., Torda, G., Bongaerts, P., Pichon, M., Parravicini, V., Hédouin, L., 2021. Mesophotic coral communities escape thermal coral bleaching in French Polynesia. R. Soc. Open Sci. 8 (11), 210139 https://doi.org/10.1098/ rsos.210139.
- Pertea, M., Pertea, G.M., Antonescu, C.M., Chang, T.-C., Mendell, J.T., Salzberg, S.L., 2015. StringTie enables improved reconstruction of a transcriptome from RNA-seq reads. Nat. Biotechnol. 33, 290–295. https://doi.org/10.1038/nbt.3122.
- Pertea, G., Pertea, M., 2020. GFF Utilities: GffRead and GffCompare. F1000Res 9, 304.

- Phillips, J.D., Gillis, D.J., Hanner, R.H., 2019. Incomplete estimates of genetic diversity within species: Implications for DNA barcoding. Ecol. Evol. 9, 2996–3010. https://doi.org/10.1002/ece3.4757
- Prada, C., Hellberg, M.E., 2013. Long prereproductive selection and divergence by depth in a Caribbean candelabrum coral. Proc. Natl. Acad. Sci. 110, 3961–3966. https://doi.org/10.1073/pnas.1208931110.
- Purcell, S., Neale, B., Todd-Brown, K., Thomas, L., Ferreira, M.A.R., Bender, D., Maller, J., Sklar, P., de Bakker, P.I.W., Daly, M.J., Sham, P.C., 2007. PLINK: A Tool Set for Whole-Genome Association and Population-Based Linkage Analyses. Am. J. Hum. Genet. 81, 559–575. https://doi.org/10.1086/519795.
- Putnam, H.M., 2021. Avenues of reef-building coral acclimatization in response to rapid environmental change. Journal of Experimental Biology 224, jeb239319. Doi: 10.1 242/jeb.239319.
- Qu, W., Liang, N., Wu, Z., Zhao, Y., Chu, D., 2020. Minimum sample sizes for invasion genomics: Empirical investigation in an invasive whitefly. Ecol. Evol. 10, 38–49. https://doi.org/10.1002/ece3.5677.
- R Core Team, R.C., 2020. R Core Team R: a language and environment for statistical computing. Foundation for Statistical Computing.
- Reich, H.G., Robertson, D.L., Goodbody-Gringley, G., 2017. Do the shuffle: Changes in Symbiodinium consortia throughout juvenile coral development. PLoS ONE 12, e0171768. Doi: 10.1371/journal.pone.0171768.
- Reynolds, J.M., Bruns, B.U., Fitt, W.K., Schmidt, G.W., 2008. Enhanced photoprotection pathways in symbiotic dinoflagellates of shallow-water corals and other cnidarians. Proc. Natl. Acad. Sci. 105, 13674–13678. https://doi.org/10.1073/ pnss.0855187105
- Risk, M., Sammarco, P., 1991. Cross-shelf trends in skeletal density of the massive coral Pontes lobata from the Great Barrier Reef. Mar. Ecol. Prog. Ser. 69, 195–200. https://doi.org/10.3354/meps069195.
- Rocha, R.J.M., Silva, A.M.B., Fernandes, M.H.V., Cruz, I.C.S., Rosa, R., Calado, R., 2014. Contrasting Light Spectra Constrain the Macro and Microstructures of Scleractinian Corals. PLoS ONE 9, e105863. Doi: 10.1371/journal.pone.0105863.
- Rocha, L.A., Pinheiro, H.T., Shepherd, B., Papastamatiou, Y.P., Luiz, O.J., Pyle, R.L., Bongaerts, P., 2018. Mesophotic coral ecosystems are threatened and ecologically distinct from shallow water reefs. Science 361, 281–284. https://doi.org/10.1126/ science.aad1614.
- Sáez-Vásquez, J., Delseny, M., 2019. Ribosome Biogenesis in Plants: From Functional 45S Ribosomal DNA Organization to Ribosome Assembly Factors. Plant Cell 31, 1945–1967. https://doi.org/10.1105/tpc.18.00874.
- Salih, A., Larkum, A., Cox, G., Kühl, M., Hoegh-Guldberg, O., 2000. Fluorescent pigments in corals are photoprotective. Nature 408, 850–853. https://doi.org/10.1038/ 25049564
- Sanford, E., Kelly, M.W., 2011. Local Adaptation in Marine Invertebrates. Annu. Rev. Mar. Sci. 3, 509–535. https://doi.org/10.1146/annurey-marine-120709-142756.
- Savolainen, O., Lascoux, M., Merilä, J., 2013. Ecological genomics of local adaptation. Nat. Rev. Genet. 14, 807–820. https://doi.org/10.1038/nrg3522.
- Schindelin, J., Arganda-Carreras, I., Frise, E., Kaynig, V., Longair, M., Pietzsch, T., Preibisch, S., Rueden, C., Saalfeld, S., Schmid, B., Tinevez, J.-Y., White, D.J., Hartenstein, V., Eliceiri, K., Tomancak, P., Cardona, A., 2012. Fiji: an open-source platform for biological-image analysis. Nat. Methods 9, 676–682. https://doi.org/10.1038/mmeth.2019
- Scucchia, F., Nativ, H., Neder, M., Goodbody-Gringley, G., Mass, T., 2020. Physiological Characteristics of Stylophora pistillata Larvae Across a Depth Gradient. Front. Mar. Sci. 7, 13. https://doi.org/10.3389/fmars.2020.00013.
- Scucchia, F., Malik, A., Putnam, H.M., Mass, T., 2021a. Genetic and physiological traits conferring tolerance to ocean acidification in mesophotic corals. Glob. Chang. Biol. 27, 5276–5294. https://doi.org/10.1111/gcb.15812.
- Scucchia, F., Malik, A., Zaslansky, P., Putnam, H.M., Mass, T., 2021b. Combined responses of primary coral polyps and their algal endosymbionts to decreasing seawater pH. Proc. Roy. Soc. B 288 (1953), 20210328. https://doi.org/10.1098/ rsnb.2021.0328
- Serrano, X., Baums, I.B., O'Reilly, K., Smith, T.B., Jones, R.J., Shearer, T.L., Nunes, F.L. D., Baker, A.C., 2014. Geographic differences in vertical connectivity in the Caribbean coral Montastraea cavernosa despite high levels of horizontal connectivity at shallow depths. Mol. Ecol. 23, 4226–4240. https://doi.org/10.1111/mec.12861.
- Serrano, X.M., Baums, I.B., Smith, T.B., Jones, R.J., Shearer, T.L., Baker, A.C., 2016. Long distance dispersal and vertical gene flow in the Caribbean brooding coral Porites astreoides. Sci. Rep. 6, 21619. https://doi.org/10.1038/srep21619.
- Shlesinger, T., Loya, Y., 2021. Depth-dependent parental effects create invisible barriers to coral dispersal. Commun. Biol. 4, 202. https://doi.org/10.1038/s42003-021-01272.9
- Smith, S.R., Sarkis, S., Murdoch, T.J.T., Weil, E., Croquer, A., Bates, N.R., Johnson, R.J., de Putron, S., Andersson, A.J., 2013. Threats to Coral Reefs of Bermuda. In: Sheppard, C.R.C. (Ed.), Coral Reefs of the United Kingdom Overseas Territories, Coral Reefs of the World. Springer Netherlands, Dordrecht, pp. 173–188. Doi: 10.1 007/978-94-007-5965-7\_13.
- Studivan, M.S., Milstein, G., Voss, J.D., 2019. Montastraea cavernosa corallite structure demonstrates distinct morphotypes across shallow and mesophotic depth zones in the Gulf of Mexico. PLoS ONE 14, e0203732. Doi: 10.1371/journal.pone.0203732.
- Studivan, M.S., Voss, J.D., 2018. Population connectivity among shallow and mesophotic Montastraea cavernosa corals in the Gulf of Mexico identifies potential for refugia. Coral Reefs 37, 1183–1196. https://doi.org/10.1007/s00338-018-1733-7.
- Studivan, M.S., Voss, J.D., 2020. Transcriptomic plasticity of mesophotic corals among natural populations and transplants of *Montastraea cavernosa* in the Gulf of Mexico and Belize. Mol. Ecol. 29, 2399–2415. https://doi.org/10.1111/mec.15495.

- Thibert-Plante, X., Hendry, A.P., 2011. The consequences of phenotypic plasticity for ecological speciation: Plasticity and ecological speciation. J. Evol. Biol. 24, 326–342. https://doi.org/10.1111/j.1420-9101.2010.02169.x.
- Trask, J.A.S., Malhi, R.S., Kanthaswamy, S., Johnson, J., Garnica, W.T., Malladi, V.S., Smith, D.G., 2011. The effect of SNP discovery method and sample size on estimation of population genetic data for Chinese and Indian rhesus macaques (Macaca mulatta). Primates 52, 129–138. https://doi.org/10.1007/s10329-010-0232-4.
- Van OPPEN, M.J.H., Bongaerts, PIM, Underwood, J.N., Peplow, L.M., Cooper, T.F., 2011. The role of deep reefs in shallow reef recovery: an assessment of vertical connectivity in a brooding coral from west and east Australia: vertical connectivity in a brooding coral. Mol. Ecol. 20 (8), 1647–1660.
- Weir, B.S., Cockerham, C.C., 1984. Estimating F-Statistics For The Analysis Of Population Structure. Evolution 38, 1358–1370. https://doi.org/10.1111/j.1558-5646.1984. tb05657.x.
- Willing, E.-M., Dreyer, C., van Oosterhout, C., 2012. Estimates of Genetic Differentiation Measured by FST Do Not Necessarily Require Large Sample Sizes When Using Many SNP Markers. PLoS ONE 7, e42649. Doi: 10.1371/journal.pone.0042649.
- Wilson, C.H., Indarto, D., Doucet, A., Pogson, L.D., Pitman, M.R., McNicholas, K., Menz, R.I., Overall, C.M., Abbott, C.A., 2013. Identifying Natural Substrates for Dipeptidyl Peptidases 8 and 9 Using Terminal Amine Isotopic Labeling of Substrates (TAILS) Reveals in Vivo Roles in Cellular Homeostasis and Energy Metabolism. J. Biol. Chem. 288, 13936–13949. https://doi.org/10.1074/jbc.M112.445841.
- Wong, K.H., Putnam, H.M., 2022. The genome of the mustard hill coral, Porites astreoides. Gigabyte 2022, 1–12. https://doi.org/10.46471/gigabyte.65.

- Young, M.D., Wakefield, M.J., Smyth, G.K., Oshlack, A., 2010. Gene ontology analysis for RNA-seq: accounting for selection bias. Genome Biol. 11, R14. https://doi.org/ 10.1186/gb-2010-11-2-r14.
- Yu, G., Lam, T.T.-Y., Zhu, H., Guan, Y., 2018. Two Methods for Mapping and Visualizing Associated Data on Phylogeny Using *Ggtree*. Molecular Biology and Evolution 35, 3041–3043. Doi: 10.1093/molbev/msy194.
- Zaslansky, P., Fratzl, P., Rack, A., Wu, M.-K., Wesselink, P.R., Shemesh, H., 2011. Identification of root filling interfaces by microscopy and tomography methods: Microtomography and microscopy observations of root fillings. Int. Endod. J. 44, 395–401. https://doi.org/10.1111/j.1365-2591.2010.01830.x.
- Zeggini, E., Rayner, W., Morris, A.P., Hattersley, A.T., Walker, M., Hitman, G.A., Deloukas, P., Cardon, L.R., McCarthy, M.I., 2005. An evaluation of HapMap sample size and tagging SNP performance in large-scale empirical and simulated data sets. Nat. Genet. 37, 1320–1322. https://doi.org/10.1038/ng1670.
- Zheng, X., Levine, D., Shen, J., Gogarten, S.M., Laurie, C., Weir, B.S., 2012. A high-performance computing toolset for relatedness and principal component analysis of SNP data. Bioinformatics 28, 3326–3328. Doi: 10.1093/bioinformatics/bts606.
- Ziegler, M., Roder, C.M., B¼chel, C., Voolstra, C.R., 2015. Mesophotic coral depth acclimatization is a function of host-specific symbiont physiology. Front. Mar. Sci. 2 https://doi.org/10.3389/fmars.2015.00004.
- Zimmerman, S.J., Aldridge, C.L., Oyler-McCance, S.J., 2020. An empirical comparison of population genetic analyses using microsatellite and SNP data for a species of conservation concern. BMC Genomics 21, 382. https://doi.org/10.1186/s12864-020-06783-9.